NBSIR 80-2008

Physical Testing of Polymers for Use in Circulatory Assist Devices

Robert W. Penn, Ph.D., Principal Investigator
Gregory B. McKenna, Ph.D., Project Leader
Fredo A. Khoury, Ph.D., Project Leader

NBSIR 80-2008

PHYSICAL TESTING OF POLYMERS FOR USE IN CIRCULATORY ASSIST DEVICES

Robert W. Penn, Ph.D., Principal Investigator
Gregory B. McKenna, Ph.D., Project Leader
Freddy A. Khoury, Ph.D., Project Leader

Polymer Science and Standards Division
National Bureau of Standards
U.S. Department of Commerce
Washington, D.C. 20234

Preface

This report presents results obtained in a research program on Physical Testing of Polymers for use in Circulatory Assist Devices carried out at the National Bureau of Standards with the support of the National Heart, Lung and Blood Institute of the National Institutes of Health. The report covers work performed in the period July 1, 1978 to September 30, 1979.

Abstract

This is the second annual report on a project directed to the
development of accelerated physical testing procedures and to the evaluation
of candidate elastomers for use in circulatory assist devices. Three
candidate materials are under study along with a standard butyl rubber.
The three candidate materials are a polyolefin rubber, a urethane-silicone
copolymer, and a segmented polyurethane elastomer. During this report
period, all of these materials have become, or are becoming, available
in adequate supply.

We report results from both uniaxial and biaxial testing with both
static and dynamic stress histories. Our results show that in static
uniaxial loading the butyl rubber is superior to the polyolefin at short
times (high stresses) but that this behavior reverses at long times (low
stresses). Under dynamic (fatigue) loading the failure times decrease
with increasing test frequency, but not rapidly enough to say that the
samples fail after a constant number of cycles. Statistical analysis of
the failure data shows that there is greater variability in the failure
times for the polyolefin rubber than for the butyl rubber in all tests
in which a comparison can be made.

Biaxial fatigue test results show that the urethane-silicone copolymer
lasts longer than the polyolefin rubber, which lasts longer than the butyl
rubber when they are compared at the same reduced pressures. For both the
polyolefin rubber and the butyl rubber, the dependence of lifetime on stress
is the same in static and fatigue loading. The butyl rubber in both cases
shows a higher stress dependence. In the case of both rubbers, the variability
in the failure times is greater in static testing than in dynamic testing.
Data for the butyl rubber and preliminary results for the urethane silicone
copolymer from biaxial fatigue tests at 23° and 37°C reflect activation

energies for the failure process of 22 kcal and 25 kcal respectively.

Creep data under uniaxial loading are reported for all four elastomers. Creep rates range from 1.7% per decade of time for the segmented polyurethane elastomer to 4% per decade for the polyolefin rubber.

Examination of the urethane-silicone copolymer by optical microscopy shows heterogeneities on a coarser scale than has been previously reported. These structures consist of flattened spheroids with their short axes perpendicular to the plane of the sheet. Their sizes parallel to the plane of the sheet vary from a few micrometers up to about 30 μm.

Table of Contents

List of Tables

List of Figures

I. Introduction

The National Heart, Lung and Blood Institute of the National Institutes of Health has been supporting the development of artificial hearts and related circulatory assist devices for approximately fifteen years. One of the current goals of this program is to develop a human implantable left ventricular circulatory assist device. This program has been divided into three interrelated projects:

1. Pump Design and Development

2. Power Systems Development

3. Biomaterials Development.

Current configurations of the pump devices include a collapsing bladder or diaphragm with a pusher plate mechanism for circulating the blood. The bladders and diaphragms as well as tubulature and valves in these devices are frequently constructed of elastomeric materials. These materials must meet rigid requirements for thrombo-resistance, bio-compatibility, and mechanical durability.

One part of the biomaterials effort is the preparation of new materials with suitable blood compatibility. This report describes efforts directed towards determining the mechanical durability of these new biomaterials. In such applications, an elastomeric bladder or diaphragm is expected to undergo cyclic stress or strain histories at a frequency of approximately one hertz for periods of many years. Test methodologies for characterizing the mechanical durability of such materials do not exist. We are developing a methodology for describing the mechanical durability of the candidate elastomers. The methodology is based on previous work using a cumulative damage rule as a framework to describe time dependent failure of glassy and semicrystalline polymers.

In the initial phase of this research, three materials were selected for beginning the study. These were a polyolefin rubber, a segmented polyurethane elastomer, and a urethane silicone copolymer. In addition, we prepared and distributed a quantity of NBS Standard Butyl Rubber to the other contractors.

This report presents preliminary results directed towards the objectives of developing test procedures and the evaluation of candidate materials for use in circulatory assist devices. The test procedures should permit the use of accelerated tests to predict and evaluate material performance over long time intervals from relatively short time tests. As a basis for this program, we use the concept of additive damage which was presented in the pevious annual report (2).

The additivity of damage framework suggests that the testing protocol be designed to look at four aspects of failure behavior:

1. Failure times under static loads

2. Failure times under dynamic loads

3. Frequency dependence of failure times in dynamic loads

4. Statistics of failure

We have been studying the failure behavior of blood pump elastomers in both uniaxial and equibiaxial states of stress using a testing and analysis protocol which includes the above four points.

Most of our data to date have been obtained for the polyolefin rubber and the standard butyl rubber with work in progress on the other elastomers. Our results show that the uniaxial failure behavior under static loads for the butyl rubber is superior to that of the polyolefin rubber at short times, but that the polyolefin rubber is superior at long times. Under fatigue loading conditions, the failure times for both rubbers decrease with

increasing test frequency. The statistical analyses of the failure data
show that the variability in the failure times for the polyolefin rubber
is greater than that for the butyl rubber. Biaxial fatigue test results
show that the urethane silicone copolymer lasts longer than the polyolefin
rubber which lasts longer than the butyl rubber when the comparison is
made at the same reduced pressures. The variability in the failure times
for the polyolefin rubber is greater than that for the butyl rubber for
both static and dynamic tests.

Data for the butyl rubber and preliminary results for the urethane silicone
copolymer from fatigue tests at 23° and 37°C reflect activation energies
for the failure process of 22 kcal and 25 kcal respectively.

Creep data under uniaxial loading are reported for all four elastomers.
Creep rates range from 1.7% per decade of time for the segmented polyurethane
elastomer to 4% per decade for the polyolefin rubber. Under biaxial
loading, data have been obtained for the butyl rubber and the polyolefin
rubber. The creep rate for the butyl rubber is 9.1% per decade of time
and for the polyolefin rubber it varies with increasing pressure from
5.1% per decade to 14% per decade over the range of reduced pressures studied.

II. Current Research

A. Test Materials

Specimens of four elastomers have been employed in this program. They
are designated as:

1. Polyolefin Rubber

2. NBS Butyl Rubber

3. Urethane-silicone Copolymer

4. Segmented Polyurethane

Table 1

Materials Received

Material	Date Received	Number of Sheets	Thickness (mils)	Size (in.)
Urethane-Silicone Copolymer	5/9/79	12	25	12 x 12
" (reject)	5/9/79	10	25	"
Urethane-Silicone Copolymer	6/27/79	15	15-18	"
"	9/25/79	35	15-18	"
"	"	15	11-14	"
" (reject)	"	50	16	"
Polyolefin	9/31/78	3	40	6 x 6
"	10/9/78	4	40	6 x 6
"	11/29/78	11	40	6 x 6
"	9/24/79	6	40	6 x 6
Segmented Polyurethane	3/30/79	2	10	7 x 11
"	"	2	30	7 x 11
"	8/9/79	2	10	"
"	"	4	30	"

4

Table 1 lists the materials received to date.

(1) Polyolefin Rubber

The polyolefin rubber is a carbon black filled poly(hexene) which is sulfur vulcanized by the Goodyear Corporation under the trade name "Hexsyn" and is subsequently extracted with an acetone-toluene mixture at the Cleveland Clinic laboratories. In clinical applications, this material is prepared with a porous surface to which is attached a blood compatible "biolized" layer. The samples supplied to date have neither the porous surface nor the blood compatible coating. Dr. Carl McMillin of Monsanto Research Corporation has been assigned the responsibility of supplying this material and further details of the preparation and characterization of this material should be available in the annual report of that group.

(2) NBS Butyl Rubber

The NBS Butyl Rubber is a standard compound prepared according to the ASTM D-3188-73 Formula 1A, using NBS Standard Reference Material 388j. It is a sulfur vulcanized synthetic isoprene-isobutylene copolymer. This formulation was chosen as a material with properties in the range of those of the candidate CAD materials and because it has a known history of good property uniformity and reproducibility. Four hundred 6-inch square sheets 0.040" thick were prepared and distributed to the three physical testing program contractors for interlaboratory comparisons.

(3) Urethane-Silicone Copolymer

The urethane-silicone copolymer is prepared by Avco-Everett Research Laboratories under their trade name "Avcothane-51". It is a block copolymer of a poly-ether urethane and a poly-siloxane. It is prepared as a prepolymer solution in a mixture of dioxane and tetrahydrofuran. Sheets of elastomer are prepared by repeatedly dipping flat plate glass mandrels in the prepolymer

5

solution until the desired thickness is obtained. The sheets are then exposed to atmospheric moisture which completes the curing of the elastomer. We have distributed a total of 65 one-foot square sheets of material which were certified by the Avco Everett Laboratory for chemical composition and thickness uniformity. In addition, we have distributed another 60 sheets of material which were rejected because of foreign inclusions, streaks or uneven thickness. These sheets are believed to be chemically satisfactory and could be used for small samples cut from unflawed areas.

(4) Segmented Polyurethane

The segmented polyurethane was prepared as a solution of polyether urethane in dimethyl acetamide by Ethicon, Inc. under the trade name "Biomer". It was fabricated into sheet form by centrifugal casting by Thoratec Laboratories Corporation. We have received 10 sheets approximately 7 x 10 inches. Dr. John Kardos of Washington University has been assigned the responsibility for acquiring and distributing this material and further details of the fabrication and chemical characteristics of this material should be available in the annual report of that group.

B. Material Failure Behavior

(1) Test Methodology

We have developed a useful methodology for describing the mechanical durability of elastomers which are candidate materials for blood pump applications. This methodology is based on previous work using a cumulative damage rule as a framework to describe time dependent failure of both glassy and semicrystalline polymers [1, 2, 3].

The concept of cumulative damage depends on the assumption that material failure is the result of damage accumulation due to stress. When the damage reaches a critical value failure occurs. The Bailey [4] criterion and the form of the rule which we will use assumes that the rate at which damage

6

accumulates is a function only of the current stress, σ. The time to fail, t_B, is related to the stress history, $\sigma(\xi)$, by the following equation:

$$\int_0^{t_B} \frac{d\xi}{\tau_B(\sigma(\xi))} = 1 \qquad (1)$$

where $\tau_B(\sigma)$ is the time to fail in constant stress experiments. Thus, each increment of time, $d\xi$ during which the load is $\sigma(\xi)$, is weighted inversely as the lifetime, $\tau_B(\sigma)$, which the specimen would have had under a constant stress, σ, and the sample should fail when the value of the integral reaches one.

The additivity of damage framework suggests that the testing protocol be designed to look at four aspects of failure behavior:

1. Failure times under static loads

The failure times under static load determine the function $\tau_B(\sigma)$ which will be used with equation 1 to predict failure behavior under other load histories.

2. Failure times under dynamic loads

The deviations of the observed failure times under dynamic loads from those predicted by equation 1 and the static load data will provide guidance for the prediction of endurance in applications.

3. Frequency dependence of failure times in dynamic loads

The additivity of damage rule predicts that failure time should be independent of test frequency and frequency dependence data to test this prediction are important in determining the validity of accelerated test methods which use high frequency test data.

4. Statistics of failure

Previous results obtained for glassy and semicrystalline polymers show that the variability in the failure times changes quite significantly

7

in going from one stress history to another. Various failure models do not make this prediction. It is important to obtain data to check the validity of these predictions.

(2) Uniaxial Testing

Uniaxial failure data have been obtained for NBS Butyl and Polyolefin rubbers. Testing of the other two elastomers has been initiated. The tests were conducted at 23 $\pm$ 1°C in air. Each specimen's width and thickness were measured prior to testing. Static data were obtained by hanging weights on samples and observing the failure time. These tests were conducted to provide a stress range of between 3 and 16 MPa. Time to failure was recorded for each specimen.

Dynamic testing was conducted using an Instron* servo-controlled hydraulic testing machine which is interfaced with a Hewlett-Packard* minicomputer for control and data acquisition. The test machine is commanded by voltages generated by the computer. Sinusoidal fatigue tests were run by generating a sinewave of 200 steps per cycle for tests run at frequencies from 2×10^{-3} to 0.09 Hz. The fatigue tests were conducted from zero to peak stresses. Peak stresses of from 6.2 to 10.3 MPa were used for the polyolefin rubber. Tests on the butyl rubber were conducted at 5.5 MPa. Statistical analyses were performed on both constant stress and fatigue data.

The static test results are depicted in a plot of the logarithm of the time to fail versus stress in Figure 1. The data were fitted by least squares to the model

$$\ln t_B = A + B\sigma \qquad (2)$$

*Certain commercial materials and equipment are identified in this paper in order to specify adequately the experimental procedure. In no case does such identification imply recommendation or endorsement by the National Bureau of Standards, nor does it imply necessarily the best available for the purpose.
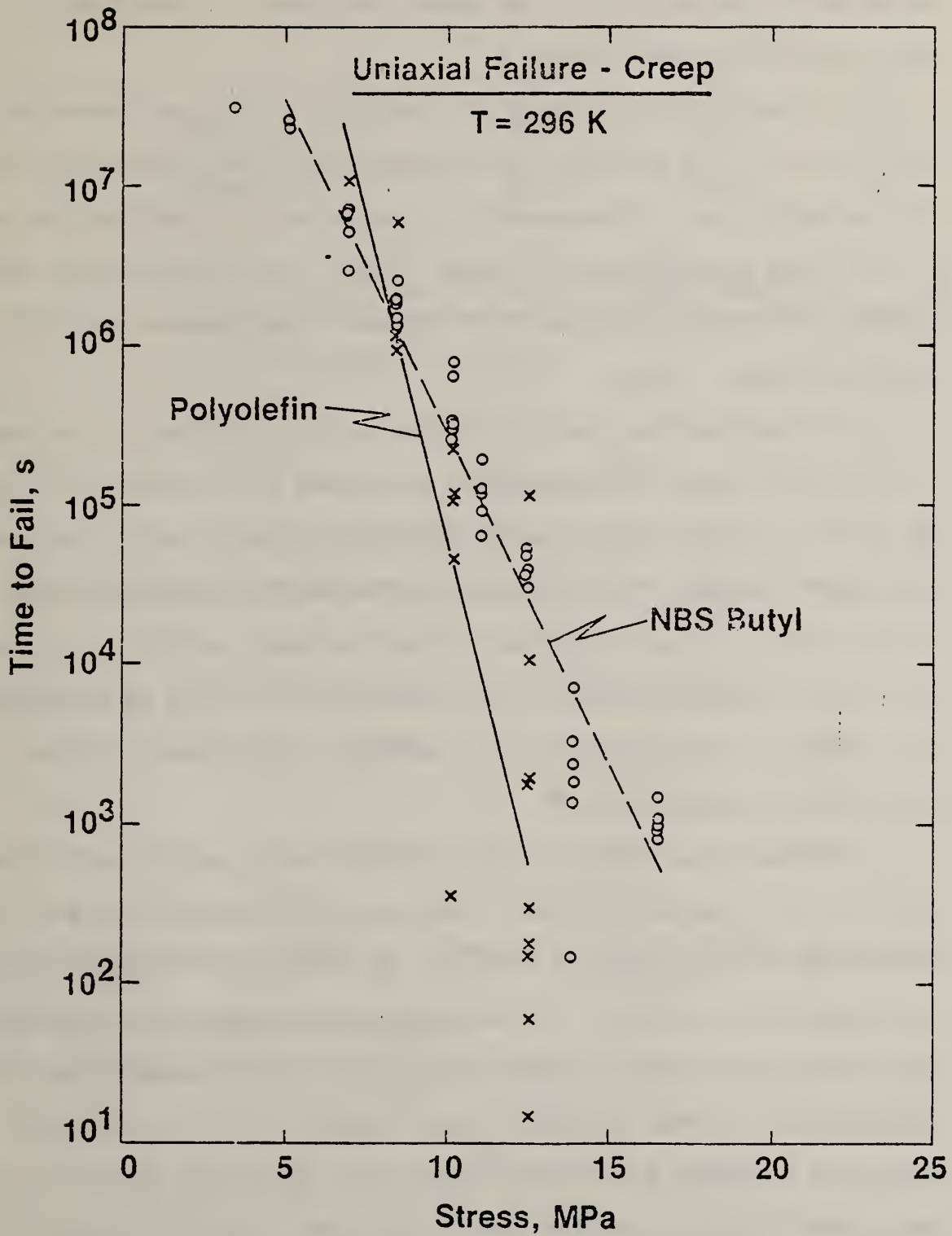
Figure 1. Time to Fail vs. Stress for NBS Butyl and Polyolefin Rubbers. Uniaxial Creep in Air at 23°C.

where t_B is the time to fail in seconds and σ is the stress in MPa. As can be seen, the fit is quite good over the stress ranges covered. The parameters determined for the two rubbers are shown in Table 2 with their correlation coefficients, R.

To illustrate the variability in the failure times, we assume that the distribution of the deviations of the logarithm of the failure times about the regression line is homoscedastic in the stress. Deviations from equation 2 are plotted as histograms in Figures 2 and 3. Both distributions appear symmetrical. That for the polyolefin rubber is much broader than that for the NBS Butyl rubber.

The assumption that the distribution of the deviations in the logarithm of the failure times is homoscedastic was tested by individually fitting the half of the data points having the highest stresses and the half having the lowest stresses. The variances from the two fits were then compared in an "F" test. We performed the "F" test for these uniaxial·static tests and for all the other uniaxial and biaxial tests for which we had 17 or more data points. In no case could the assumption of homoscedasticity be rejected at the 95% confidence level.

The dynamic test data for the polyolefin rubber were fitted to equation 2 by the least squares technique. The resulting parameters and correlation coefficients are displayed in Table 3. The results for the polyolefin rubber are summarized in Figure 4. As can be seen, the dynamic test lifetimes are much shorter than those predicted by the additivity of damage rule, and the lifetimes are a strong function of test frequency which is contrary to the additivity of damage prediction. We note that the slopes (B in eq. 2) for the dynamic test data are considerably lower than those for the static tests.

To further illustrate the frequency dependence of the fatigue lifetimes, we cross plot the dynamic test data in Figure 5 together with the results for NBS Butyl rubber. The logarithm of the time to fail, t_B, is plotted versus the logarithm of the test frequency, ω. We show

Table 2

Time to Fail Parameters for Uniaxial Static Tests*

	A	B	R	N
NBS Butyl	22.05	-.951	-.962	39
Polyolefin	29.44	-1.848	-.877	20

*Fit to $\ln t_B = A + B\sigma$ where t_B is the time to fail in seconds, and σ is the stress in MPa, and R is the coefficient of correlation. N is the number of samples.

Table 3

Least Squares Parameters for Polyolefin Uniaxial Dynamic Tests*

FREQUENCY, Hz	A	B	R	N
0.002	18.36	-.773	-.989	6
0.01	17.31	-.854	-.828	14
0.09	14.56	-.689	-.732	15

*Fit to $\ln t_B = A + B\sigma$ where t_B = time to failure in seconds and σ is the peak stress in MPa.

R is the coefficient of correlation.
N is the number of samples.
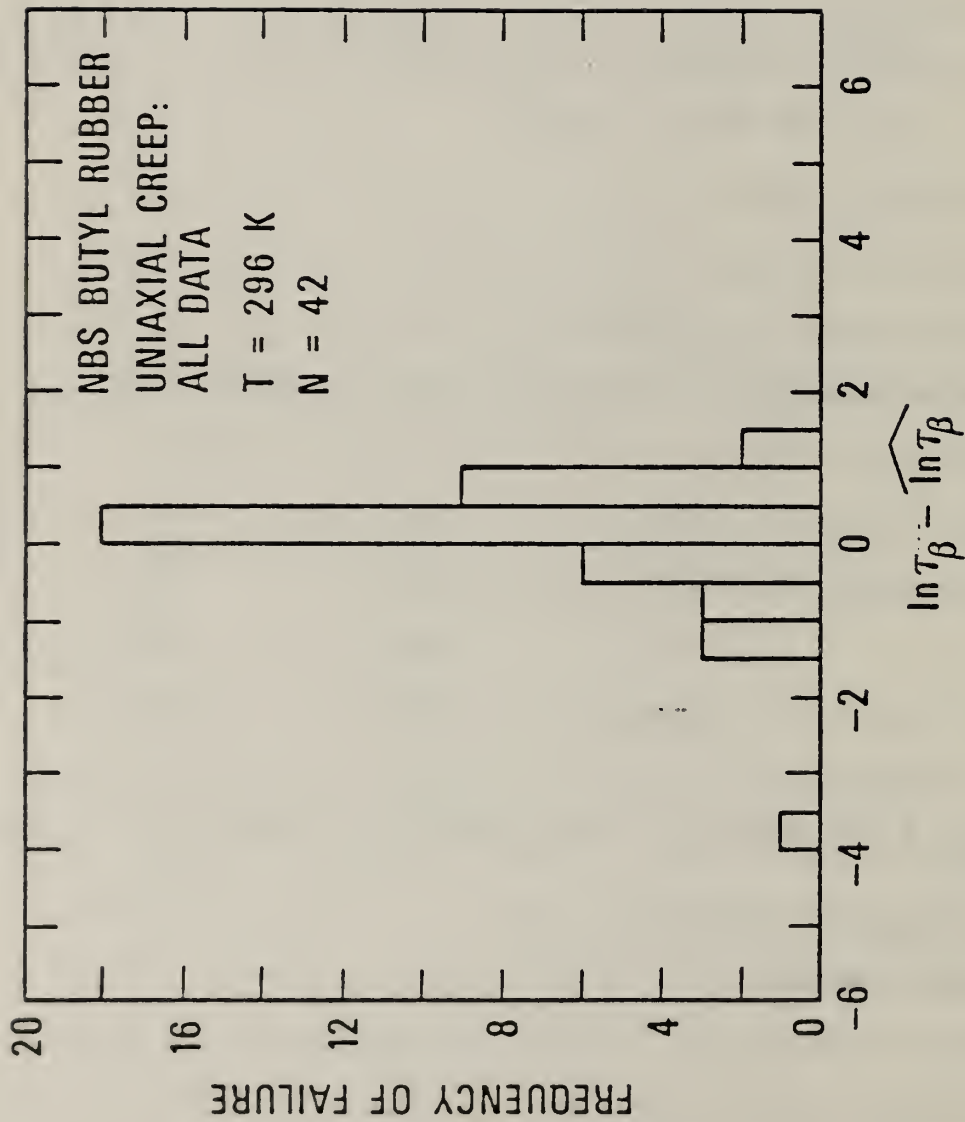
Figure 2. Histogram of Deviations from Least Squares Line for NBS Butyl Rubber in Uniaxial Creep to Failure Tests. In Air at 23°C.
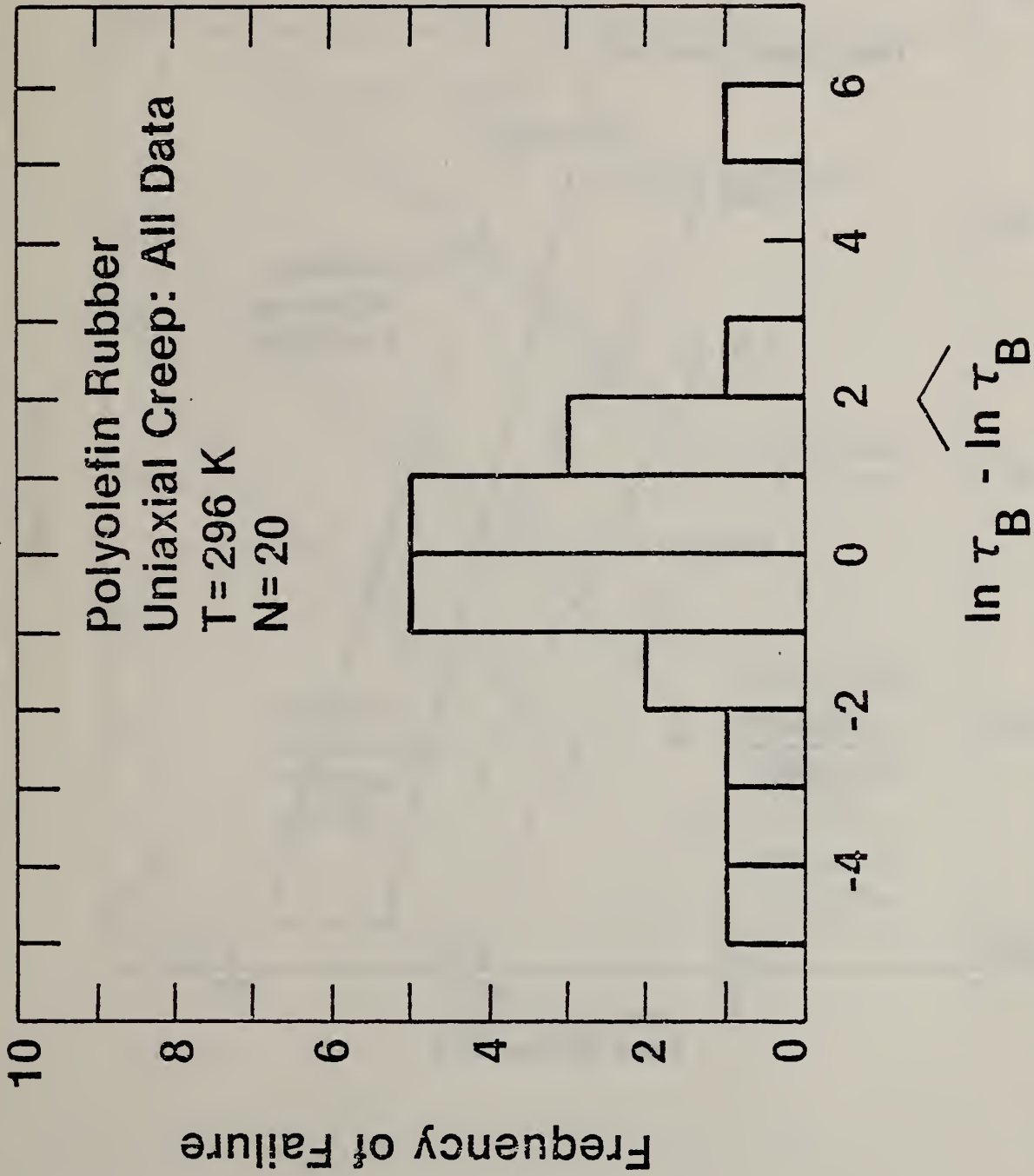
Figure 3. Histogram of Distribution of Deviations from Least Squares Line for Polyolefin Uniaxial Creep Data. In Air at 23°C.
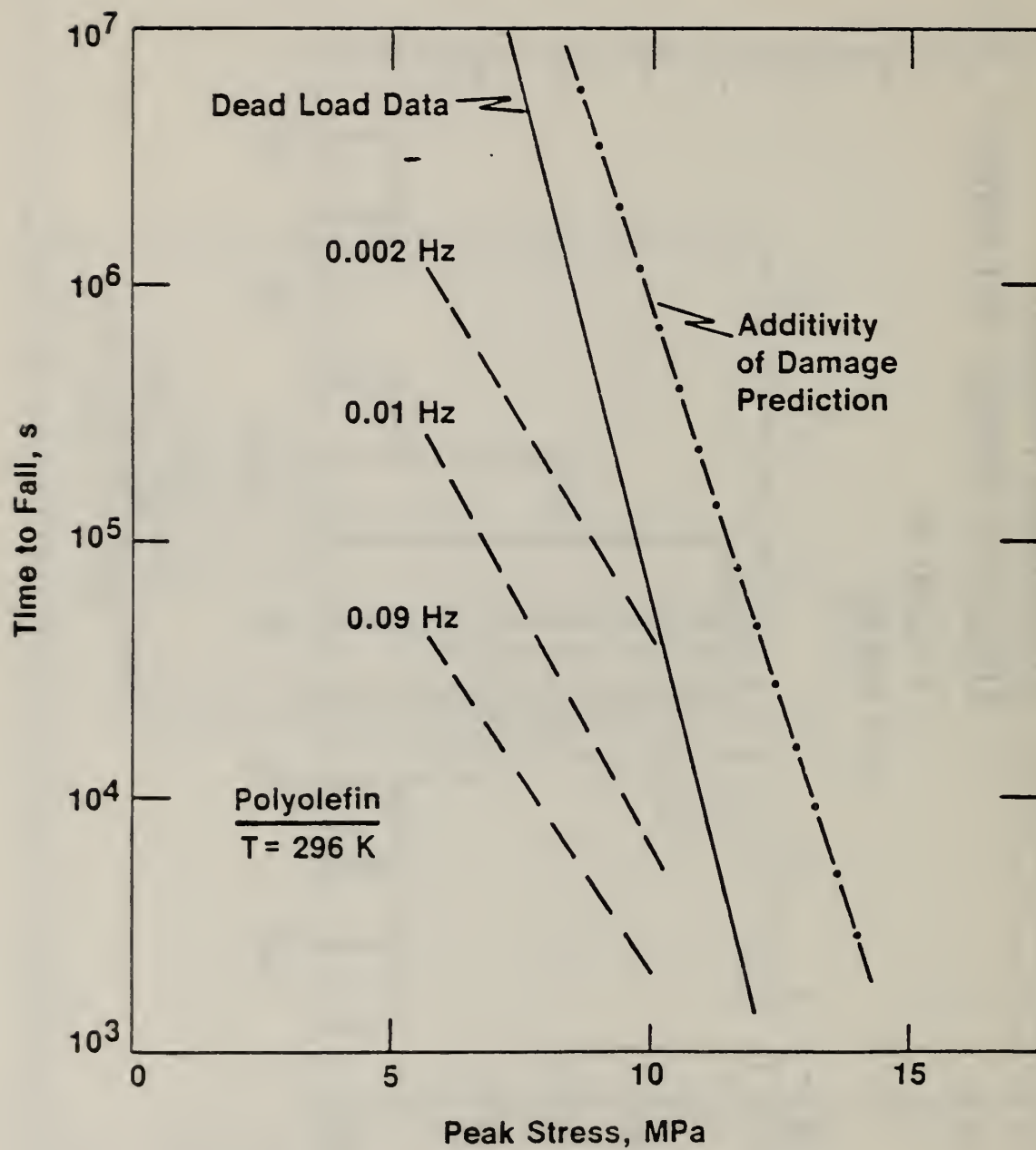
Figure 4. Time to Fail vs. Peak Stress for Uniaxial Fatigue of Polyolefin Rubber.
In Air at 23°C.
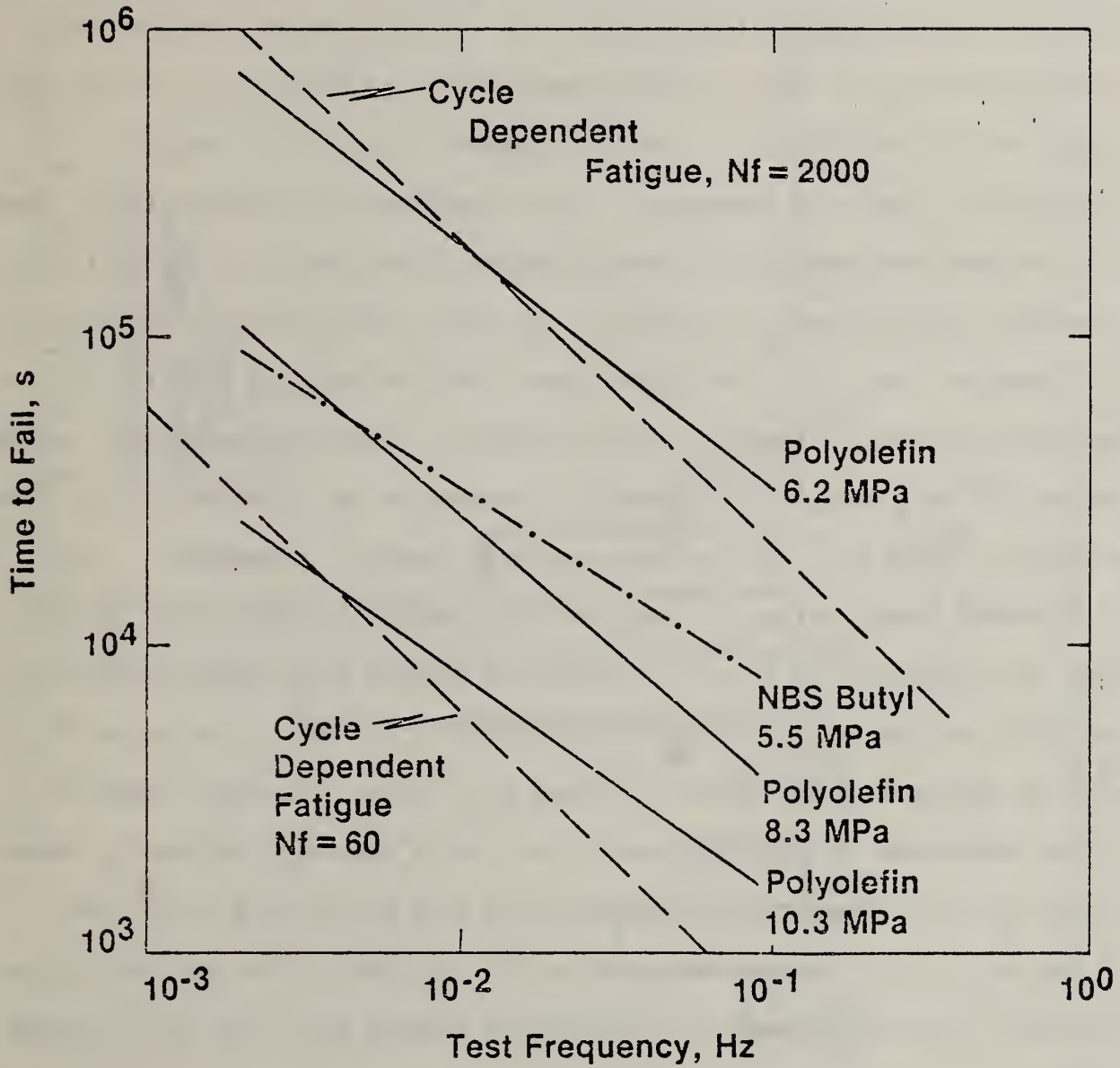
Figure 5.   Time to Fail vs. Test Frequency for NBS Butyl and Polyolefin Rubbers.
Uniaxial Fatigue in Air at 23°C.

only the least squares lines. These dynamic (fatigue) data were fit to a
multiple regression model of the form

$$\ln t_B = A + B\ln \omega + C\sigma \qquad (3)$$

The statistics were used to examine the hypothesis that fatigue failure
in the two carbon black filled rubbers is a "cycle dependent process" (i.e.
fatigue failure is a result of the accumulation of damage due to cycling the
rubber and failure occurs at a constant number of cycles, N_f, which is
independent of the test frequency. This is opposed to the additivity of damage
model we have been examining in which damage accumulates with time at a rate
dependent upon the level of stress and for which fatigue failure would occur
at a constant time, t_B). The coefficients from the model of equation (3)
are shown with their standard errors in Table 4. The standard error of estimate
for the fit is 0.391 with 32 degrees of freedom for the polyolefin data. Note that
we obtain a slope of -.748 for the polyolefin frequency dependence. This
is different from a value of -1 at the 97.5% confidence level. For the NBS
Butyl data, we obtain a slope of -.644 which differs significantly from -1 at
the 99.9% confidence level based on the student's "t" test. The value of -1
would be obtained if the material failure occurred at a constant number of
cycles independent of test frequency (i.e. "cycle dependent fatigue"). These
slopes are also significantly different from zero which would be obtained
if the additivity of damage rule were valid. Obviously, the behavior of the
polyolefin and butyl rubbers is intermediate between that predicted by these two
models.

The distribution of the deviations of the logarithm of the failure
times for the polyolefin rubber about the model of equation 2 is shown in
Figure 6. The distribution is somewhat narrower than that from the static
uniaxial data and appears skewed to the left. Insufficient data were obtained
to construct a histogram from the NBS Butyl rubber uniaxial dynamic test results.
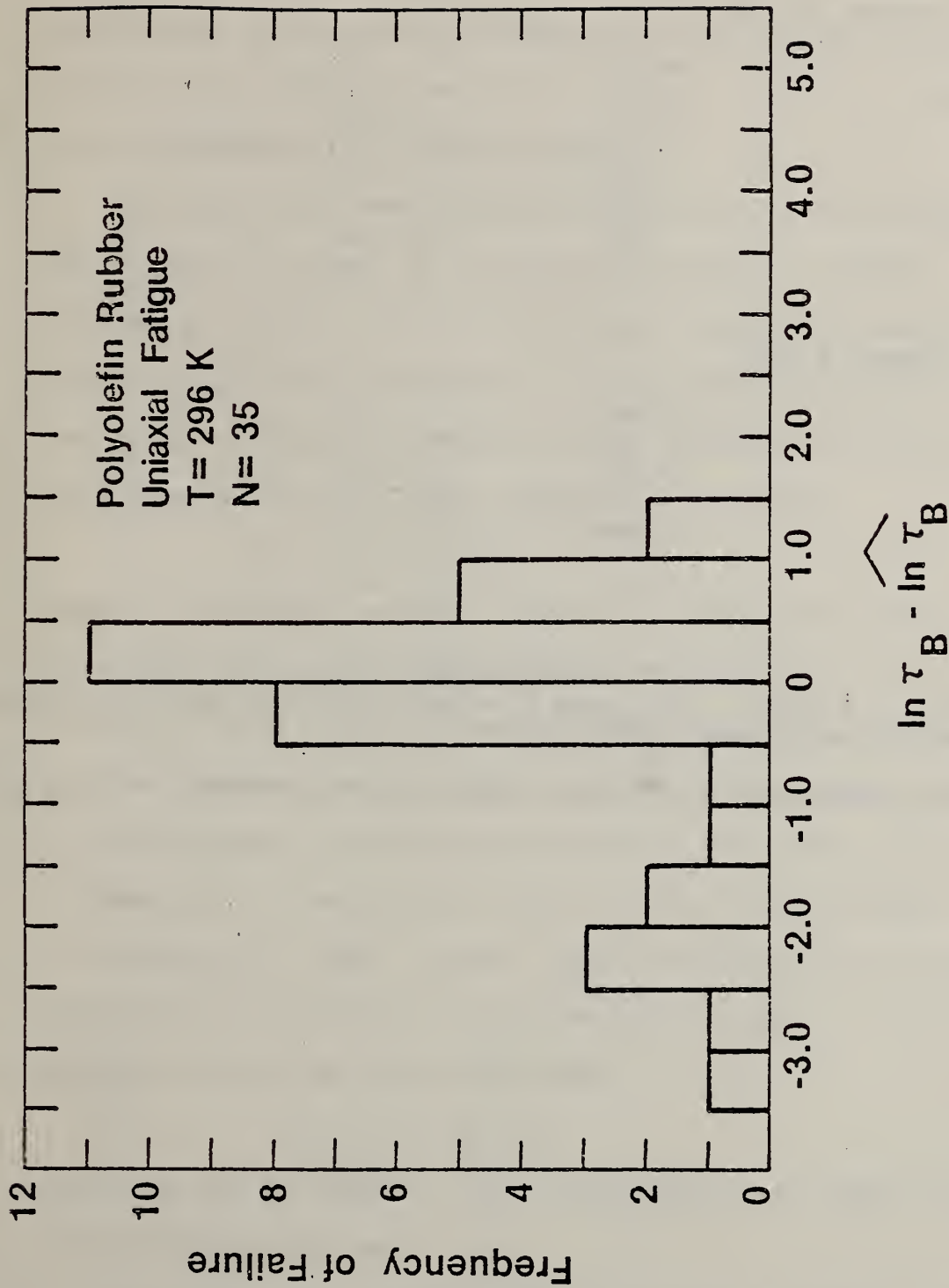
Figure 6. Histogram of Distribution of Deviations from Least Squares Line for Polyolefin Rubber Under Uniaxial Fatigue Loading. In Air at 23°C.

17

Table 4

Time to Fail Parameters for Uniaxial Dynamic Tests*

Polyolefin Rubber, N = 35

Parameter	Value	E_s
A	13.244	$\pm$ .928
B	-.748	$\pm$ .107
C	-.755	$\pm$ .101

NBS Butyl Rubber, N = 11

Parameter	Value	E_s
A	7.41	$\pm$ 0.187
B	-.644	$\pm$ .519
C	--	--

*Fit to $\ln t_B = A + B \ln \omega + C\sigma$, where t_B = time to fail in seconds, ω = frequency in Hz and σ = peak stress in MPa.

E_s is the standard error of the coefficient and N is the number of data points.

(3) Biaxial Testing

Biaxial static test data have been obtained for the NBS Butyl and the polyolefin rubbers at room temperature in air. Testing of the other two elastomers has been initiated. Biaxial dynamic data have been obtained for the NBS Butyl and polyolefin rubbers and for the urethane-silicone copolymer at 23°C and at 37°C in normal saline solution. Testing has been initiated on the segmented polyurethane elastomer.

The static data were obtained by inflating a circular membrane which was clamped at its edge using constant regulated air pressure. The apparatus is shown in Figure 7. Time to failure was recorded for each specimen. The static test results are depicted in a plot of the logarithm of time to fail versus reduced pressure (pressure divided by specimen thickness) in Figure 8. The data were fitted by linear regression to the model:

$$\ln t_B = A + B \, P/h \tag{4}$$

where t_B is the time to fail in seconds and P/h is the reduced pressure in kilo pascals per millimeter. The parameters determined for the two rubbers are included in Table 5 with the standard errors from the regression line.

To illustrate the statistics of failure in these tests, we show histograms of the deviations from the model (equation 4) in Figures 9 and 10. The distribution for the polyolefin rubber is significantly broader than that for the NBS Butyl rubber. However, some of the spread of the polyolefin data might be attributable to different lots of rubber. This effect was tested by fitting the data to the model:

$$\ln t_B = A + B\frac{P}{h} + CN$$

where N is the lot number 1 or 2. The parameter C was found to be insignificantly different from zero.

The dynamic data were obtained by inflating a circular membrane which was clamped at its edge between two glass flange joints using pressure pulses varying between zero and a peak pressure P at a frequency of three Hertz.

19
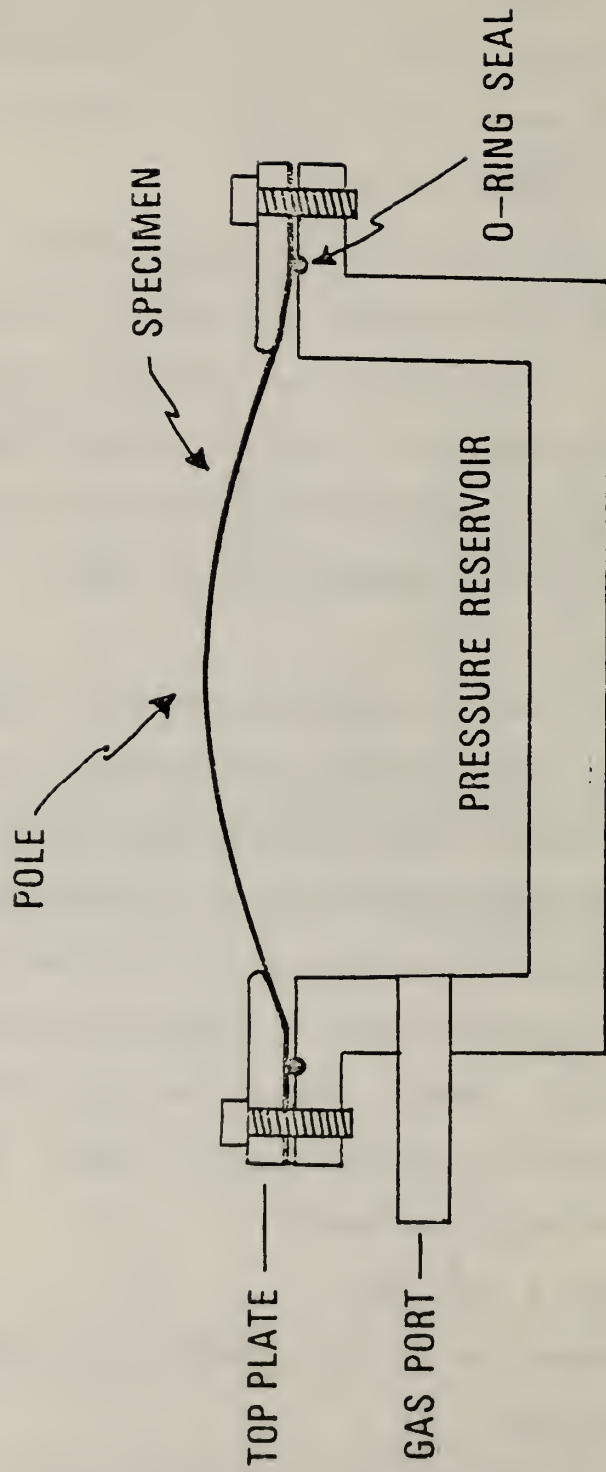
Figure 7. Schematic of Apparatus Used for Equi-biaxial Creep and Failure Measurements by Inflation of a Rubber Membrane.
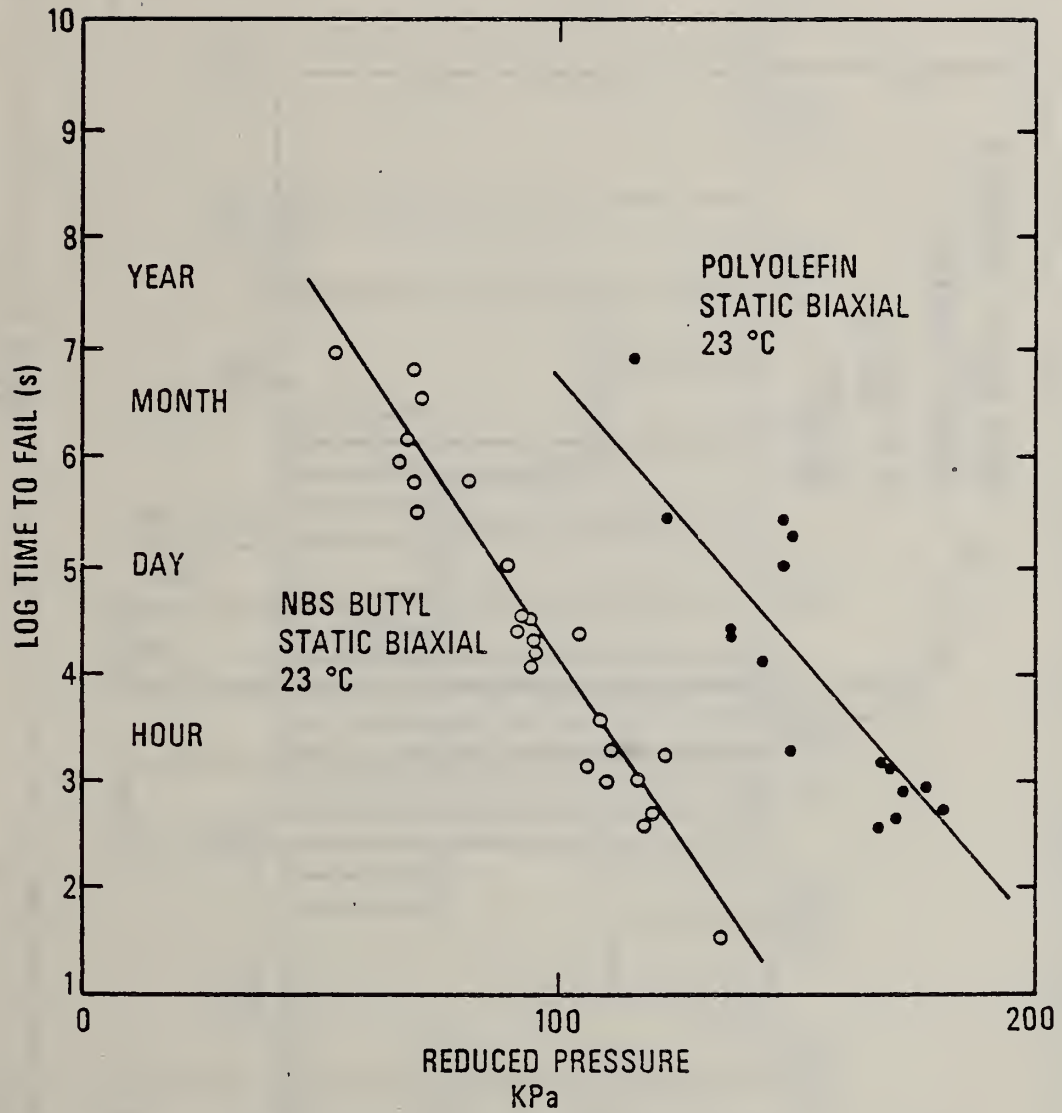
Figure 8. Time to Fail Versus Reduced Pressure for Biaxial Static Tests.
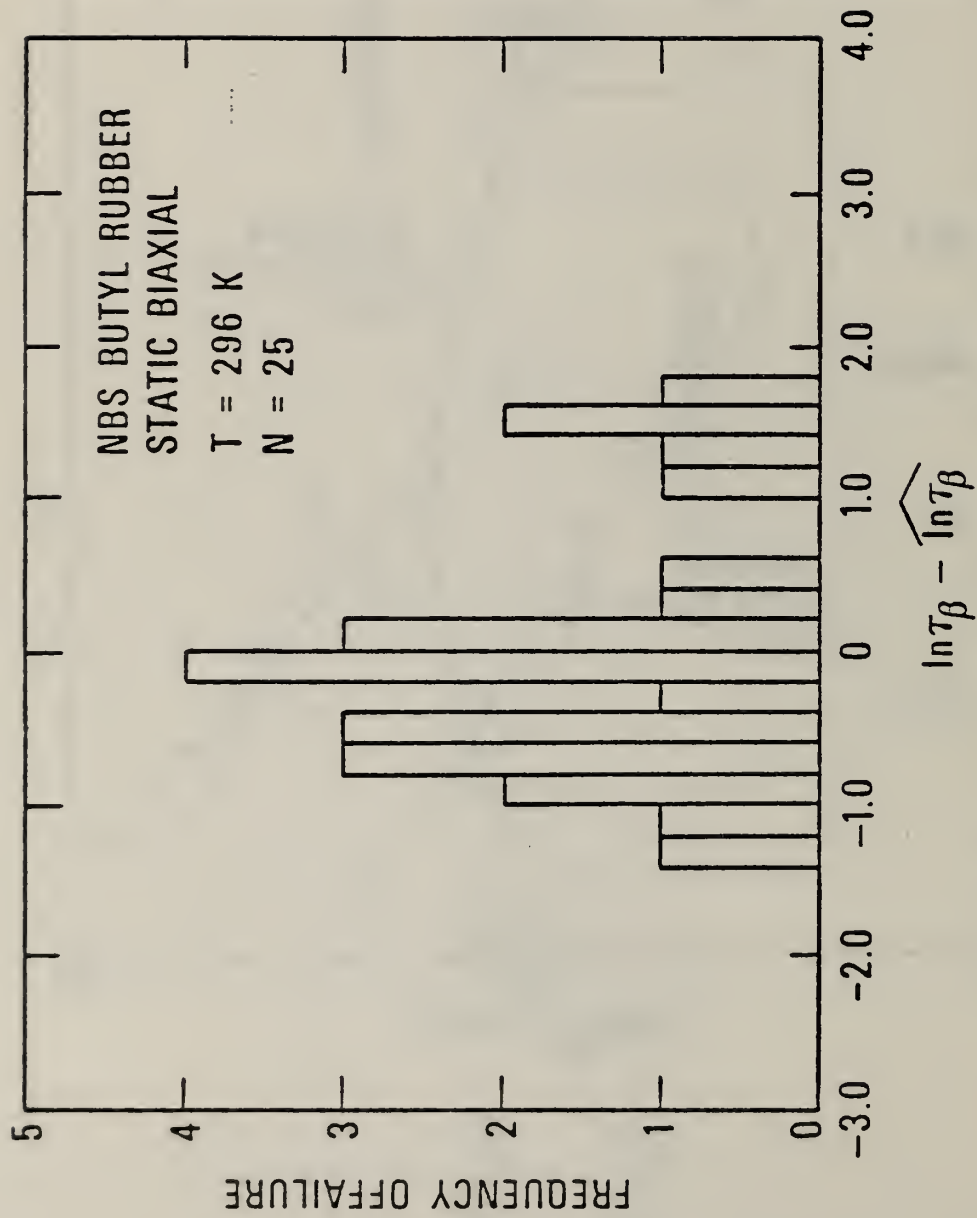
Figure 9. Histogram of Distribution of Deviations from Least Squares Line for NBS Butyl Rubber Static Biaxial Data. In Air at 23°C.
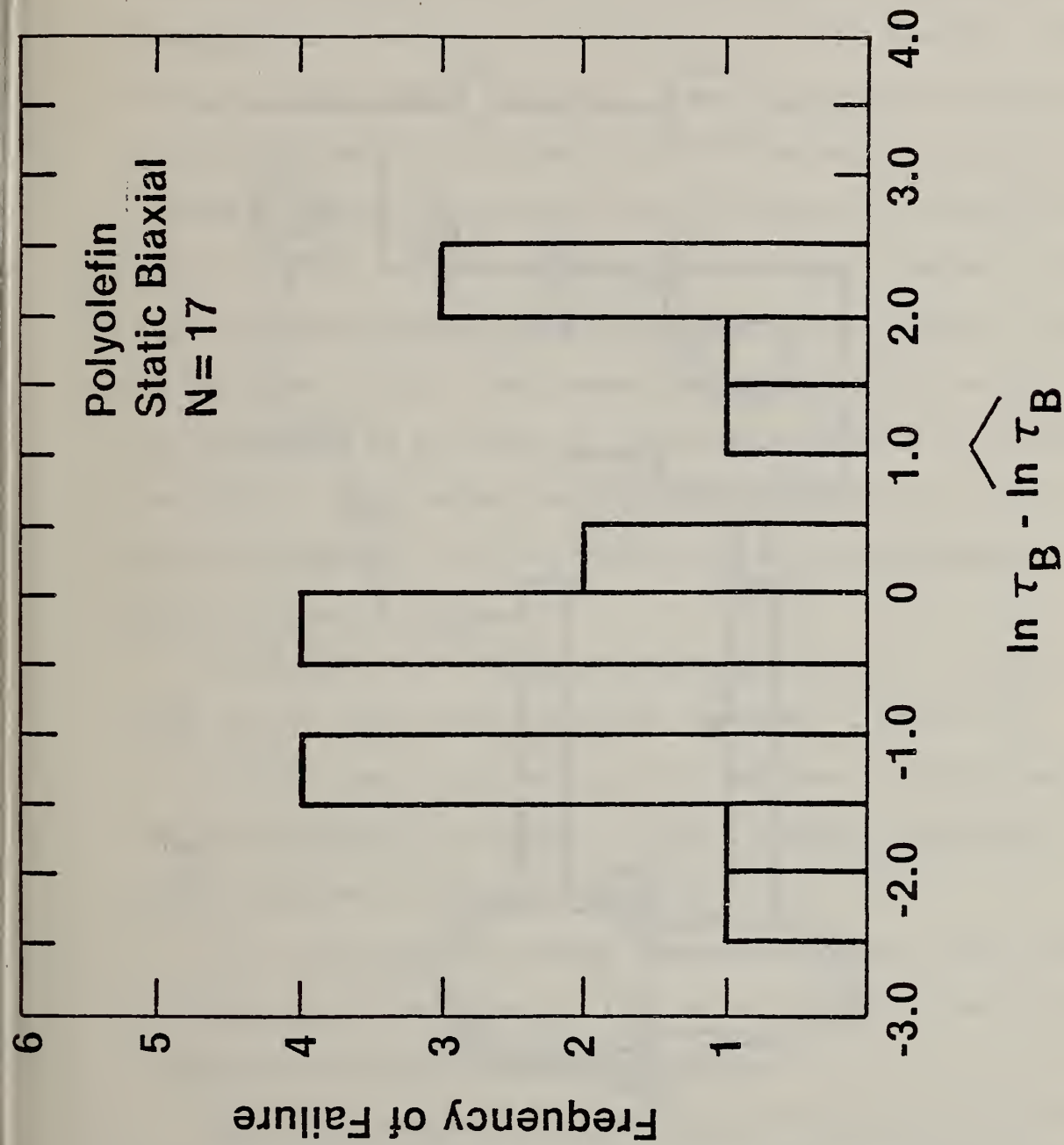
Figure 10. Histogram of Distribution of Deviations from Least Squares Line for Polyolefin Rubber Biaxial Static Data. In Air at 23°C.

23
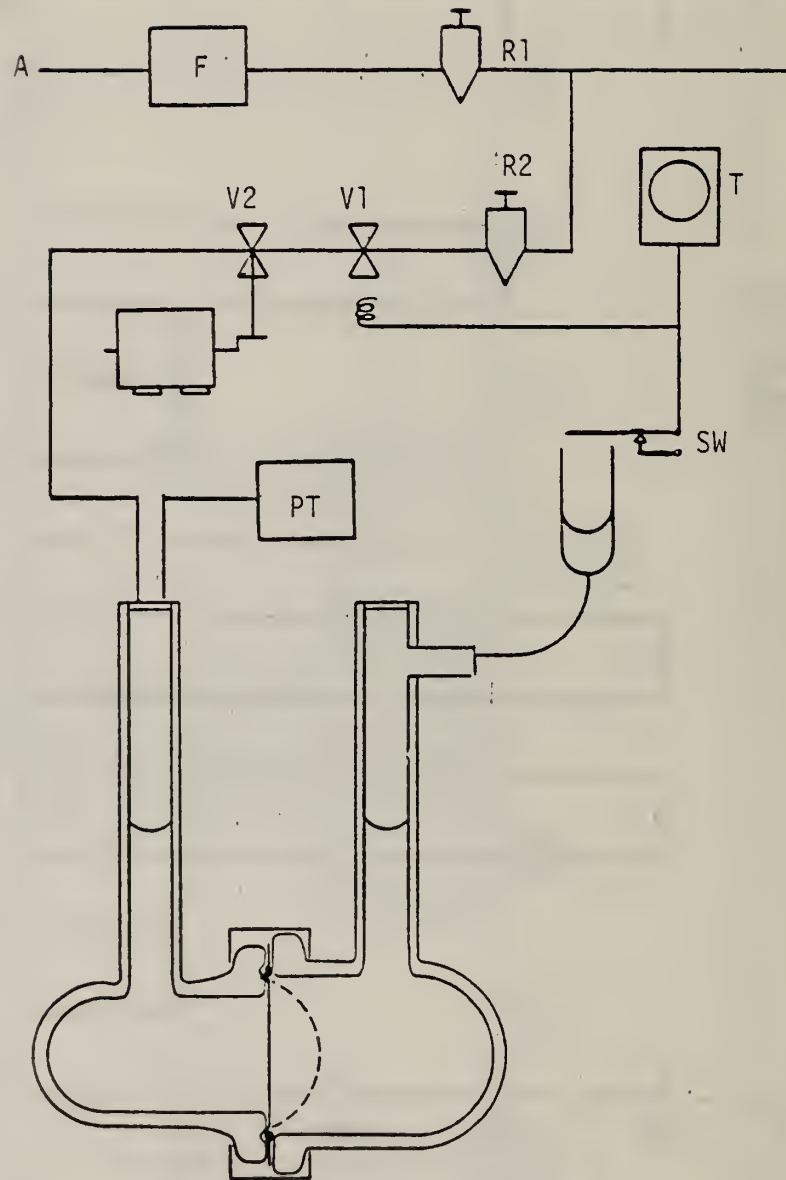
Figure 11. Dynamic Biaxial Test Apparatus. A, Air Supply. F, Filter. PT, Pressure Transducer. R1, Primary Pressure Regulator. R2, Pressure Regulator. V1, Solenoid Valve. V2, Motor Driven Spool Valve. SW, Condom Activated Microswitch. T, Timer.

The cells formed by the glass flange joints were filled with physiological saline solution. A diagram of the apparatus is shown in Figure 11. One side of the test cell is alternately connected to a regulated air pressure line and vented to the atmosphere by means of a motor driven spool valve. The peak air pressure in the cell is monitored with a pressure transducer interfaced to a rectifier circuit with a large time constant. Upon sample failure, a latex condom inflates to trip a micro-switch which turns off the running time meter and a solenoid valve in the pressure supply line. The latex condoms also serve as barriers to retard evaporation of the physiological saline solution. Time to fail is recorded for each specimen. A foamed poly-styrene float is placed in the low pressure side of the cell to prevent sloshing of the saline solution. Measurements of the peak height of this float permit the calculation of the volume of the inflated membrane to estimate the stress and strain in the specimens as discussed in reference 2. Six of these test cells were operated in air at 23°C and six more were immersed in a water bath maintained at 37°C.

The dynamic test results are depicted in plots of the logarithm of the time to fail versus reduced pressure in Figures 12 through 16.

The data were fitted to equation 4 by linear regression analysis. The resulting parameters are shown in Table 5. Several significant features may be observed in these statistics:

(1), The slopes (or pressure dependences) are not significantly different in static and dynamic testing. This is in contrast to the results obtained in uniaxial testing on the polyolefin rubber.

(2), The slopes are not significantly different at 23 and 37°C for the two materials for which data are available. This fact allows us to calcu-late activation energies for the fatigue failure process. For the NBS Butyl rubber, we obtain an activation energy of 22 kcal/mole and for the urethane-silicone copolymer we obtain 25 kcal/mole.

(3), The slopes are significantly different for the different

25
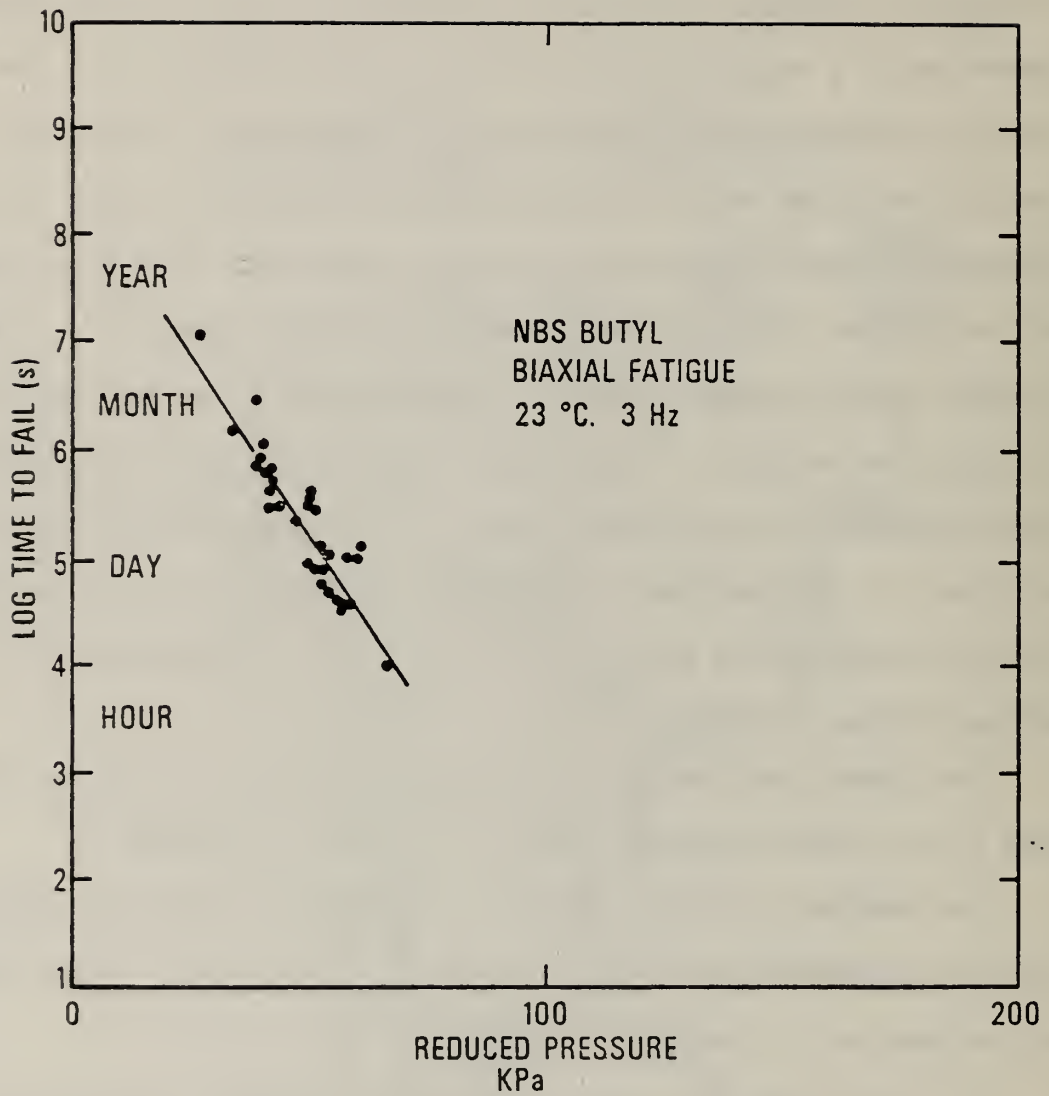
Figure 12. Time to Fail Versus Peak Reduced Pressure for Dynamic Biaxial Tests of NBS Butyl Rubber at 23°C.
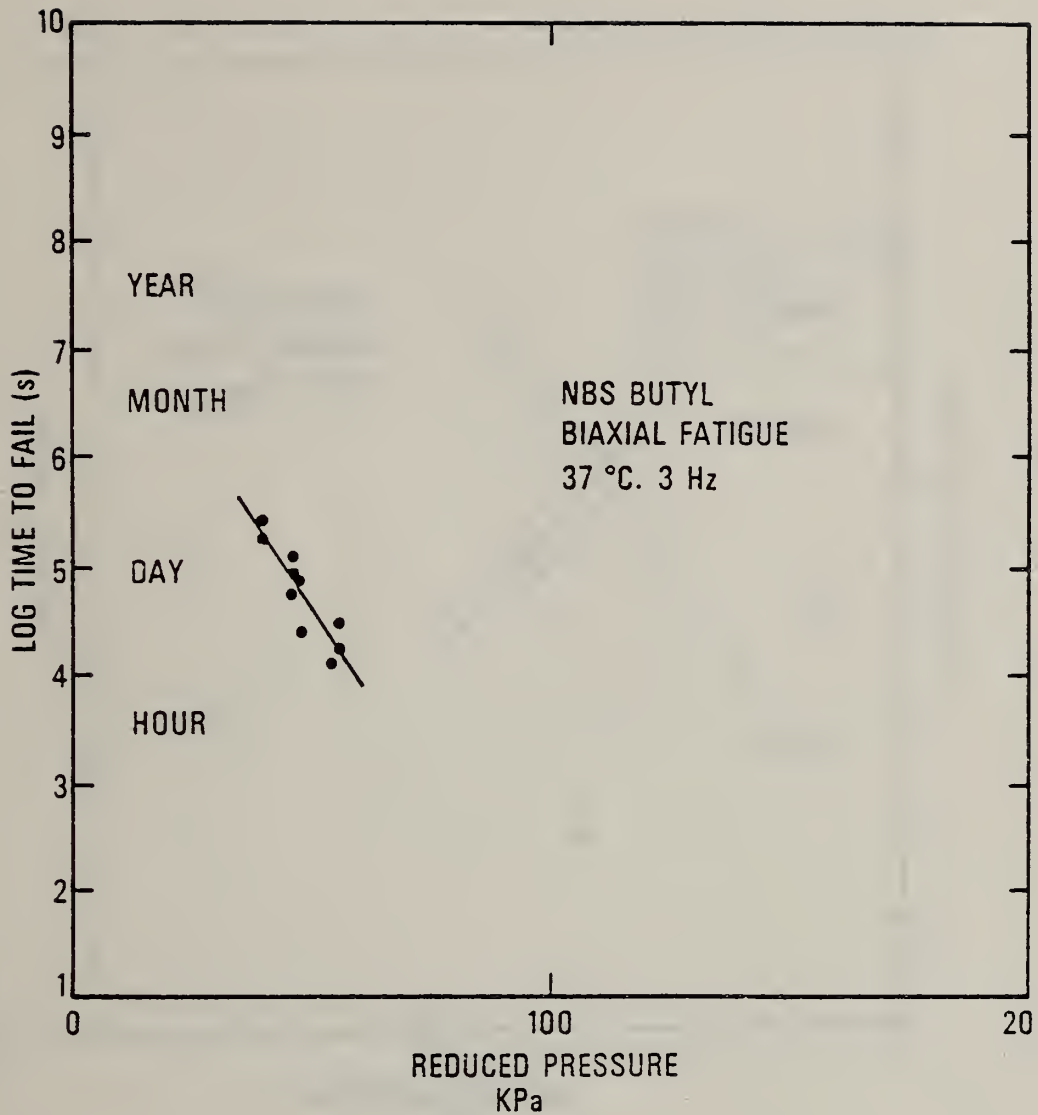
Figure 13. Time to Fail Versus Peak Reduced Pressure for Dynamic Biaxial Tests of NBS Butyl Rubber at 37°C.
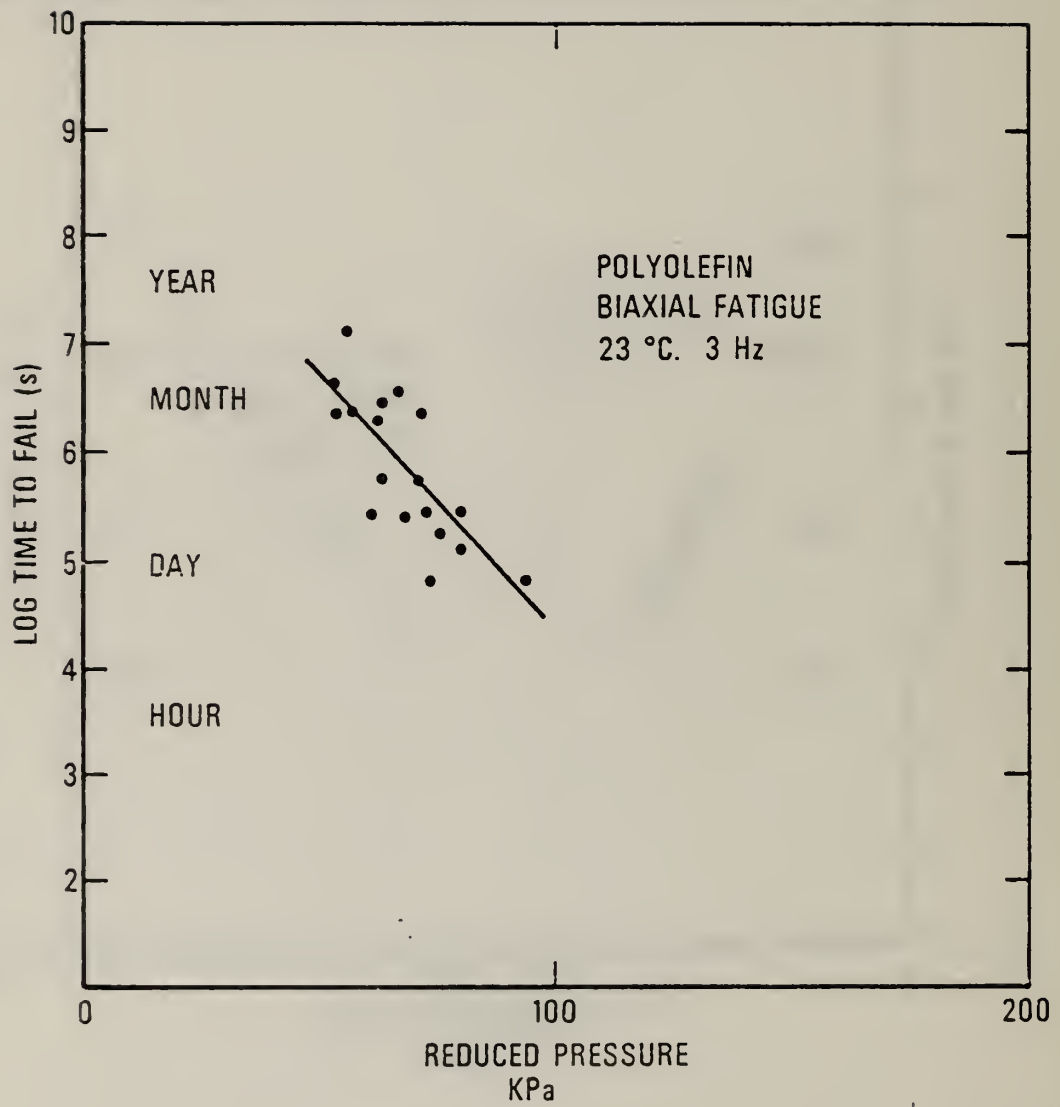
Figure 14. Time to Fail Versus Peak Reduced Pressure for Dynamic Biaxial Tests of Polyolefin Rubber at 23°C.
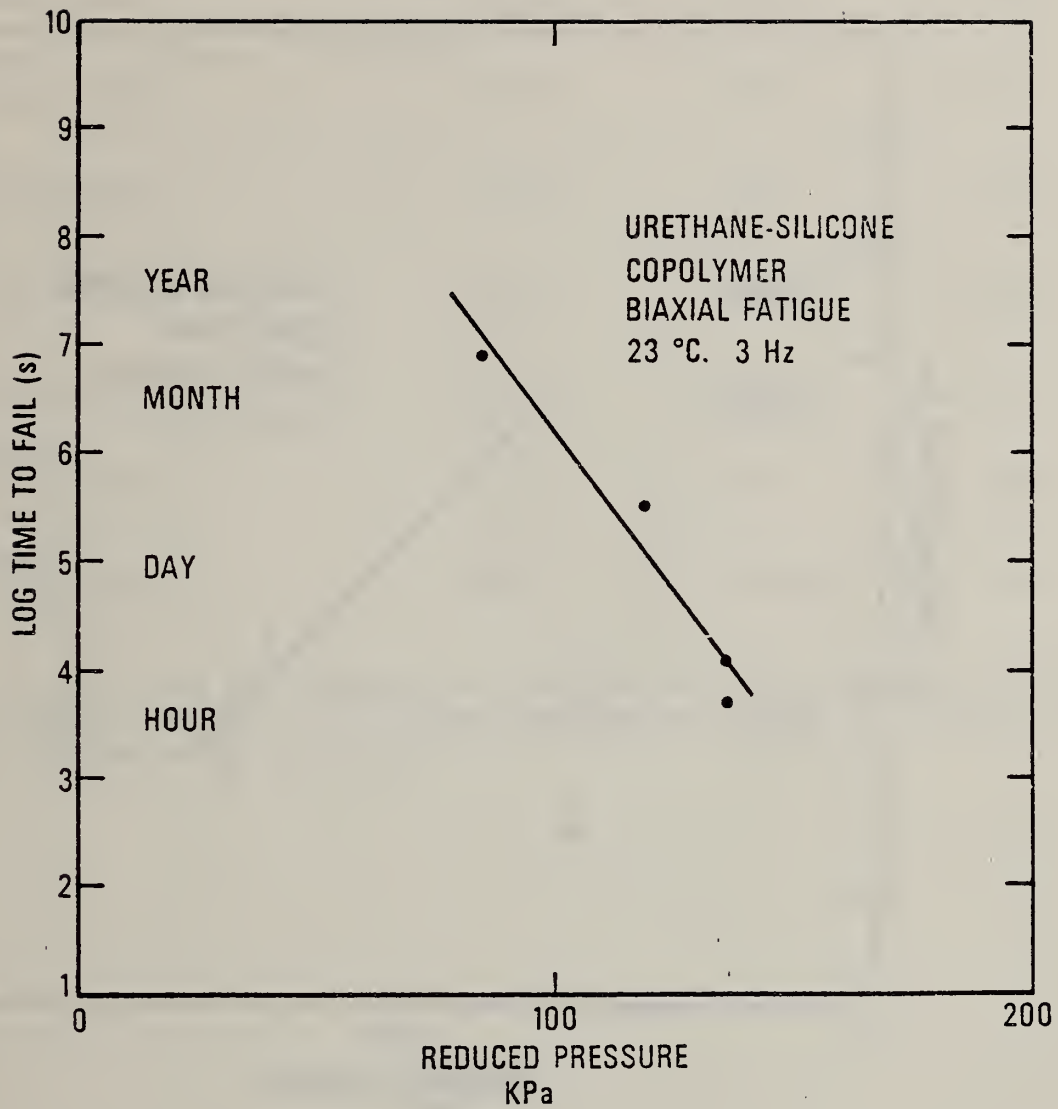
Figure 15. Time to Fail Versus Peak Reduced Pressure for Dynamic Biaxial Tests of Urethane-Silicone Copolymer at 23°C.
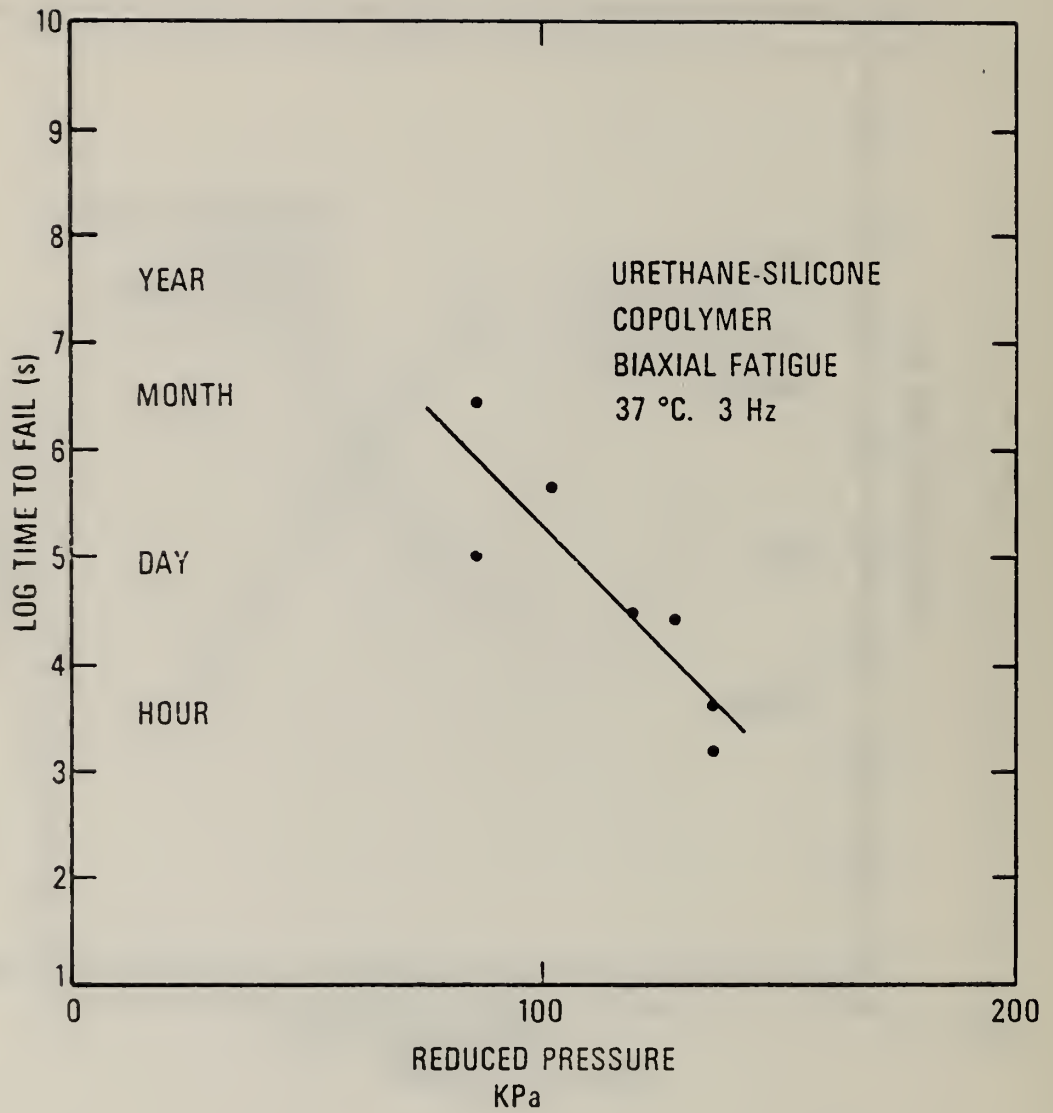
Figure 16. Time to Fail Versus Peak Reduced Pressure for Dynamic Biaxial Tests of Urethane-Silicone Copolymer at 37°C.

Table 5
Regression Parameters for Biaxial Tests*

	A	B	E_s	N
NBS Butyl Static Biax. 23°C	24.62	-.154	± .863	25
Polyolefin Static Biax. 23°C	27.20	-.118	± 1.55	17
NBS Butyl Biax. Fatigue 23°C	19.68	-.153	± .619	33
NBS Butyl Biax. Fatigue 37°C	18.33	-.156	± .491	10
Polyolefin Biax. Fatigue 23°C	20.94	-.110	± 1.01	19
US Copolymer Biax. Fatigue 23°C	27.79	-.136	± .980	4
US Copolymer Biax. Fatigue 37°C	22.52	-.104	± 1.34	7

*Fit to $\ln t_B = A + B\ P/h$, where t_B is the time to fail in seconds and P/h is the reduced pressure in kPa. E_s is the standard error from the regression line and N is the number of data points.

materials.

(4), The lifetimes are very much shorter in dynamic testing than in static testing when they are compared at the same reduced pressure. This seriously conflicts with the concept of simple linear additive damage.

(5), The variances of the distribution of deviations are significantly different at the 95% confidence level between static and dynamic loading for both the NBS Butyl and the polyolefin rubbers in biaxial testing.

To illustrate the statistics of failure in these tests, we show histograms of the deviations from equation 4 for the NBS Butyl rubber and the polyolefin rubber at room temperature. These histrograms are shown in Figures 17 and 18.

C. Creep Behavior of Candidate Elastomers

(1) Background

One aspect of the suitability of elastomers for blood pump applications is their resistance to time dependent deformation i.e., creep. In this program, we have been studying the creep behavior of the four candidate elastomers under uniaxial and equi-biaxial load conditions. The data which we have obtained to date are from tests conducted at 23°C in air. Work has recently been initiated at 23°C and 37°C in saline solution. Future work will include testing at 50°C in saline solution.

There are reasons for characterizing the material thoroughly at ambient conditions (i.e. 23°C in air). The first is that it is easier to characterize the material behavior at ambient conditions and, therefore, establish a data base for understanding the basic material creep behavior. Second, by studying changes in material behavior upon changing conditions to saline solution, higher temperature, etc, one can obtain a separate measure of chemical and mechanical effects on the deformation of the rubber. Such comparisons and their significance have been extensively

32
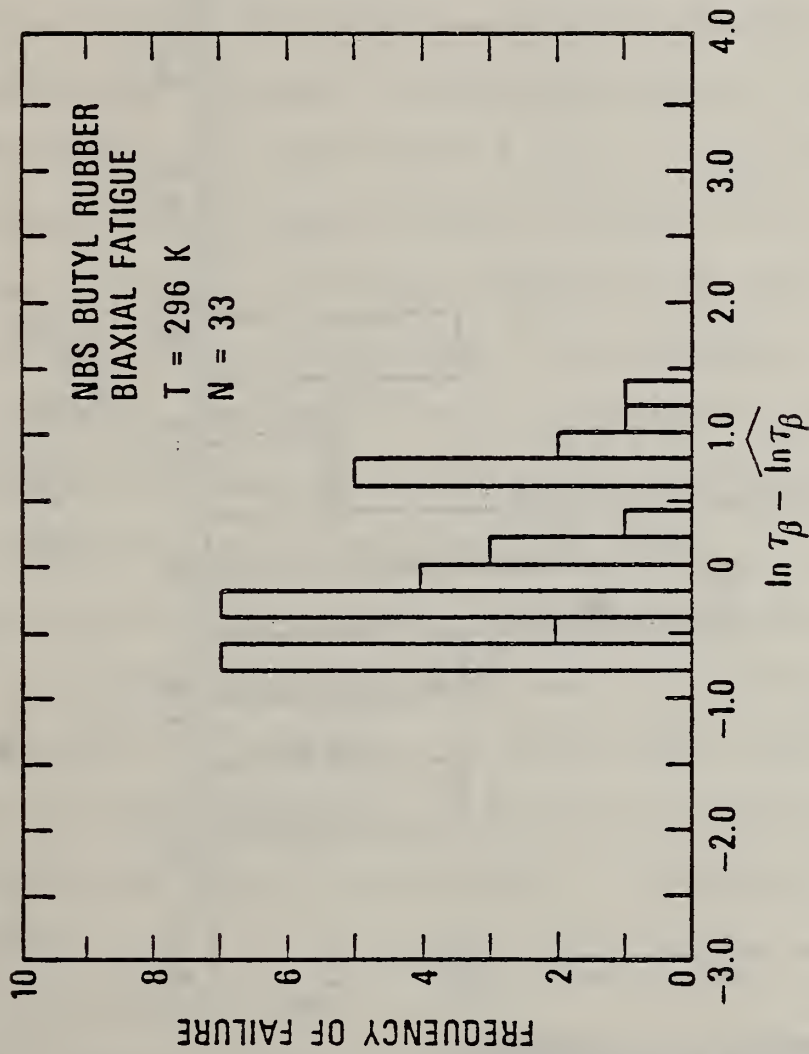
Figure 17. Histogram of Deviations from Least Squares Line for NBS Butyl Rubber Equi-biaxial Fatigue Data. In Saline Solution at 23°C.
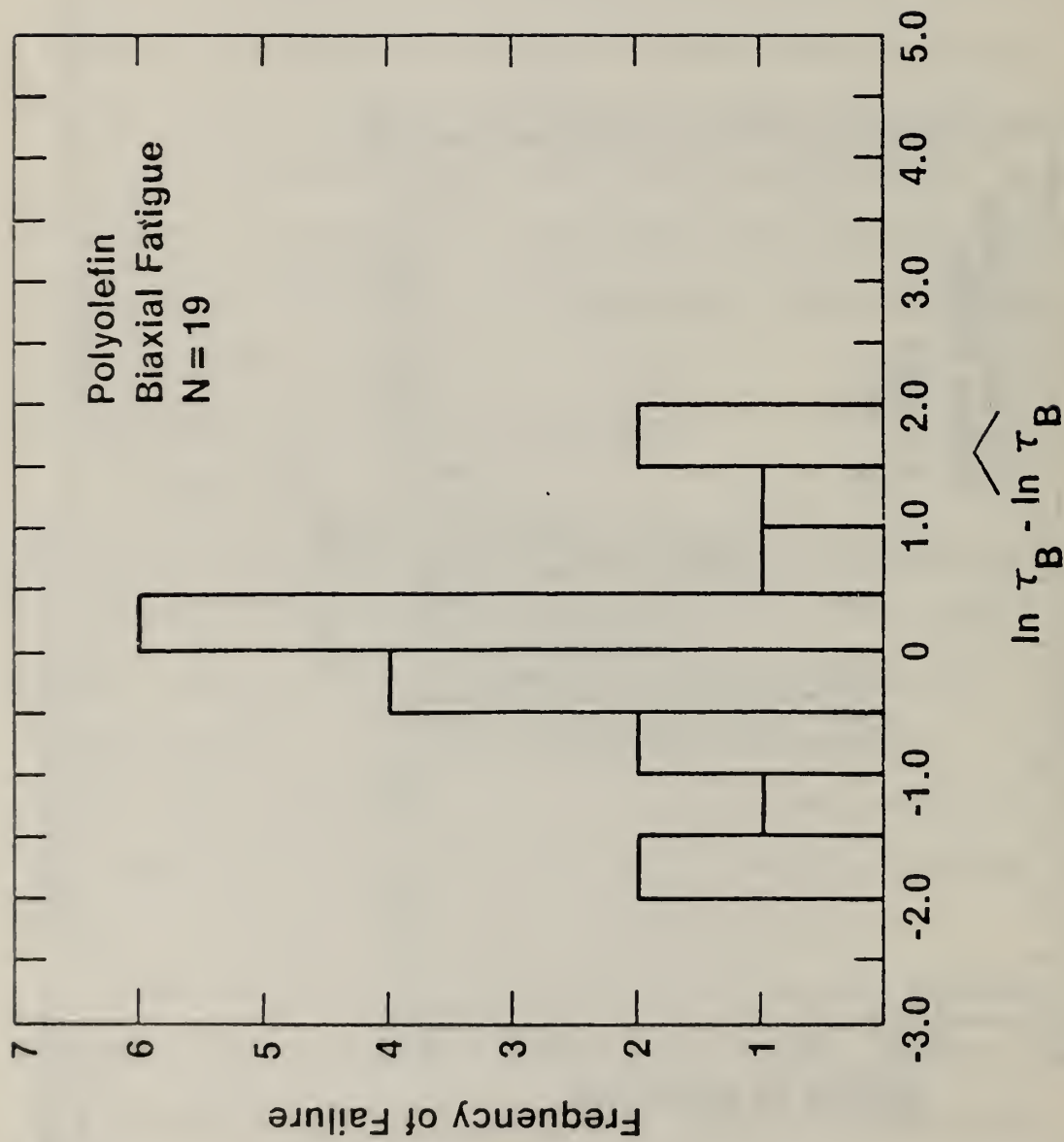
Figure 18. Histogram of Distribution of Deviations from Least Squares Line for Polyolefin Rubber Biaxial Fatigue Data. In Saline at 23°C.

34

discussed by Wood [5] in his work on natural rubber.

(2) Uniaxial Creep

Uniaxial creep of the four candidate elastomers is being measured
by applying a constant force to dumbbell specimens and measuring the
separation of gage marks on the specimens with a cathetometer. As shown
in Figures 19 through 22, the creep of the four candidate elastomers
plots as nearly straight lines on log strain vs. log time plots.
Further, we see that the lines are parallel for different stress levels.
Thus, one can easily compare the deformation behavior of the four elastomers.
Since the data are straight lines on a log ε vs. log t plot, we fit
least squares lines through the data of the form $\ln \varepsilon = A + n \ln t$. Since n is
the slope of the log ε-log t plot it represents the rate of creep, and
so serves as a useful representation of the resistance of each material
to time dependent deformation. Table 6 tabulates the average values of
n obtained for each material. As can be seen, the polyolefin shows the
highest creep rate and the polyurethane the lowest.

Future work in this area will include obtaining data at longer
times for the materials at room temperature in air, testing in saline solution at
room temperature, 37°C and 50°C. We remark, again, that comparisons of
behavior with room temperature, air testing will provide a basis for
understanding how the saline environment is affecting the candidate
elastomers.

(3) Equi-biaxial Creep

Equi-biaxial creep data are being obtained on the candidate elastomers
by applying an internal pressure to inflate a membrane. Figure 7 shows
a schematic drawing of the device. The state of deformation at the pole
of the membrane is one of equi-biaxial stretch. At the edge of the
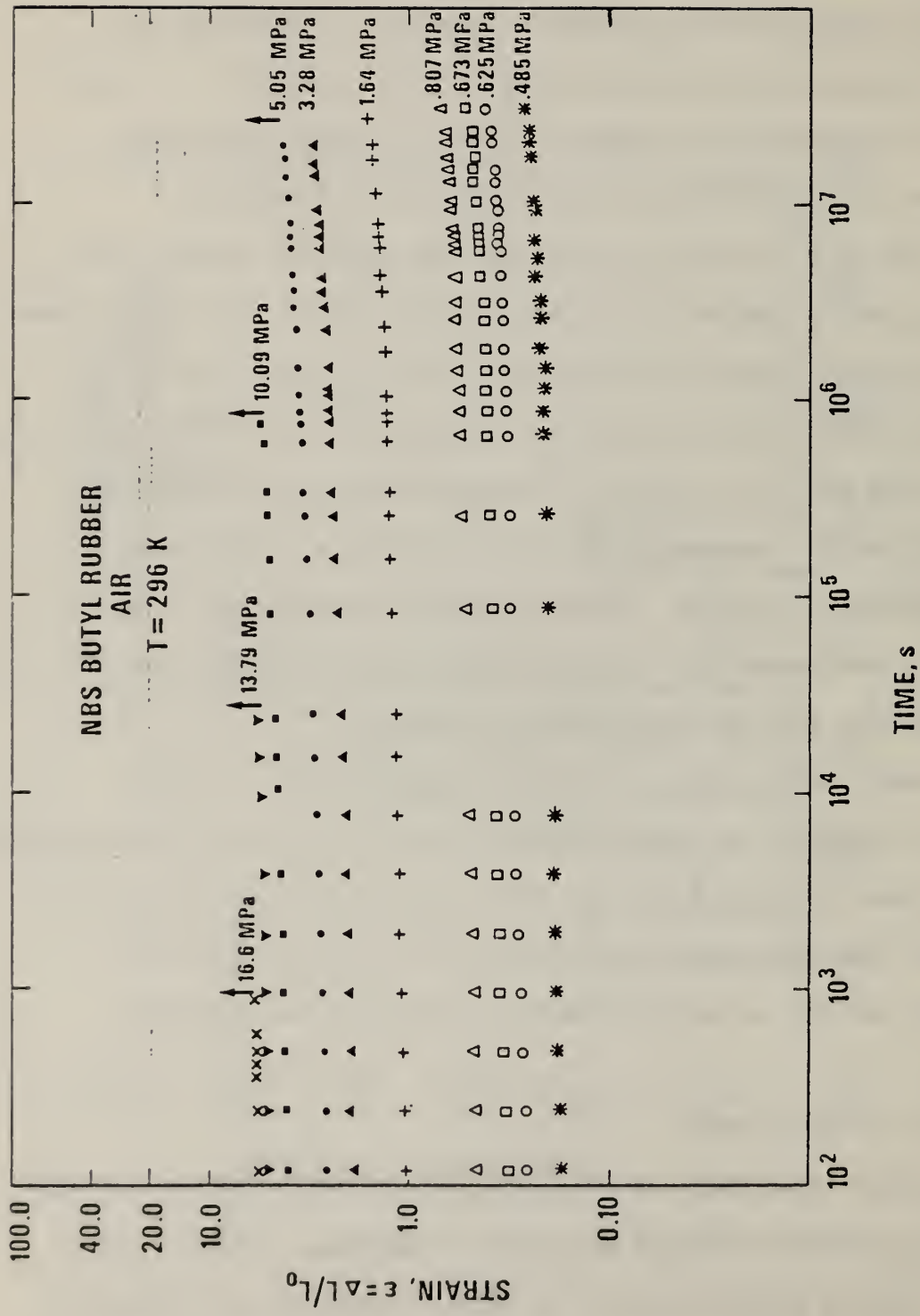
Figure 19. Uniaxial Creep of NBS Butyl Rubber. In Air at 23°C.
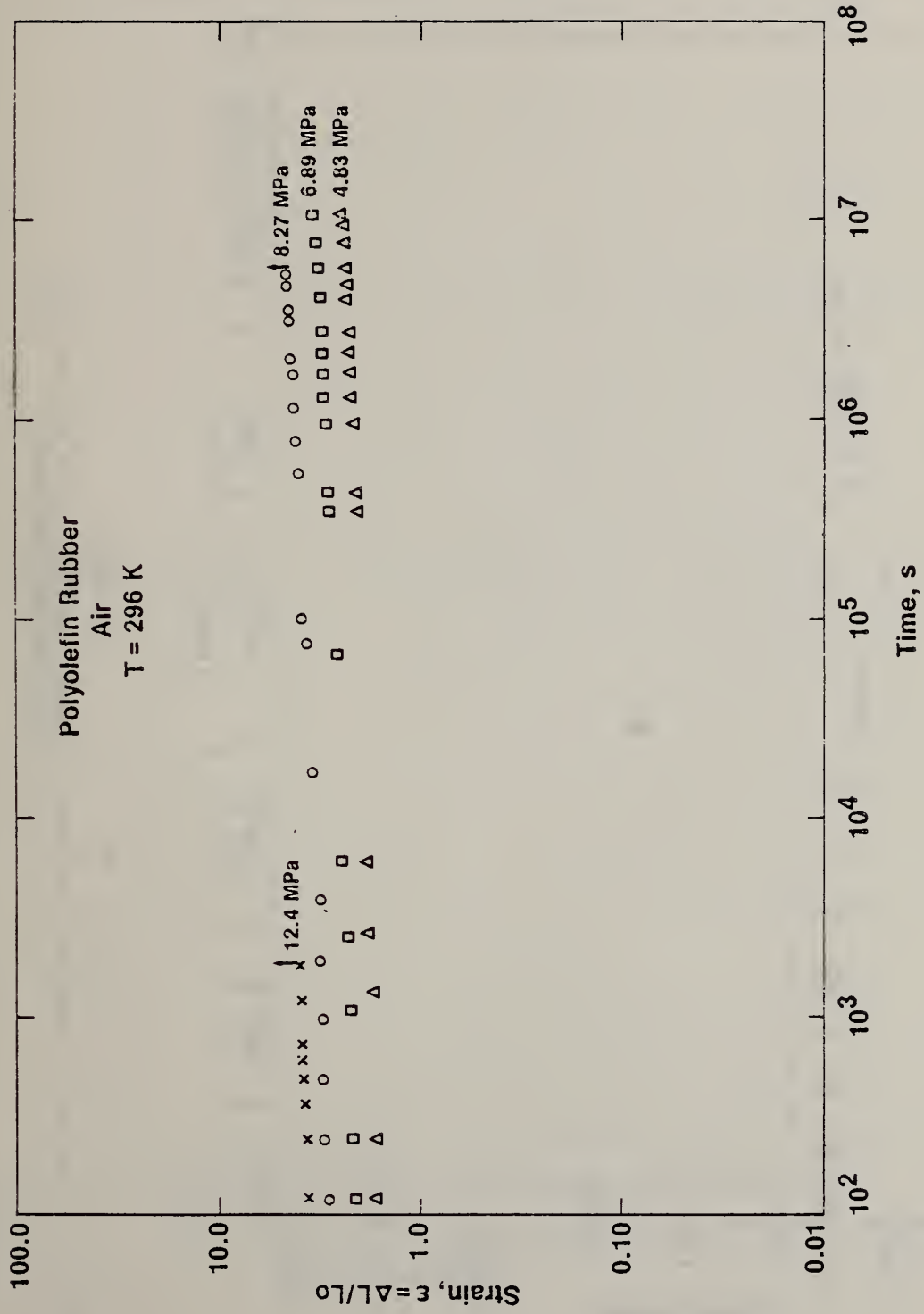
Figure 20. Uniaxial Creep of Polyolefin Rubber. In Air at 23°C.
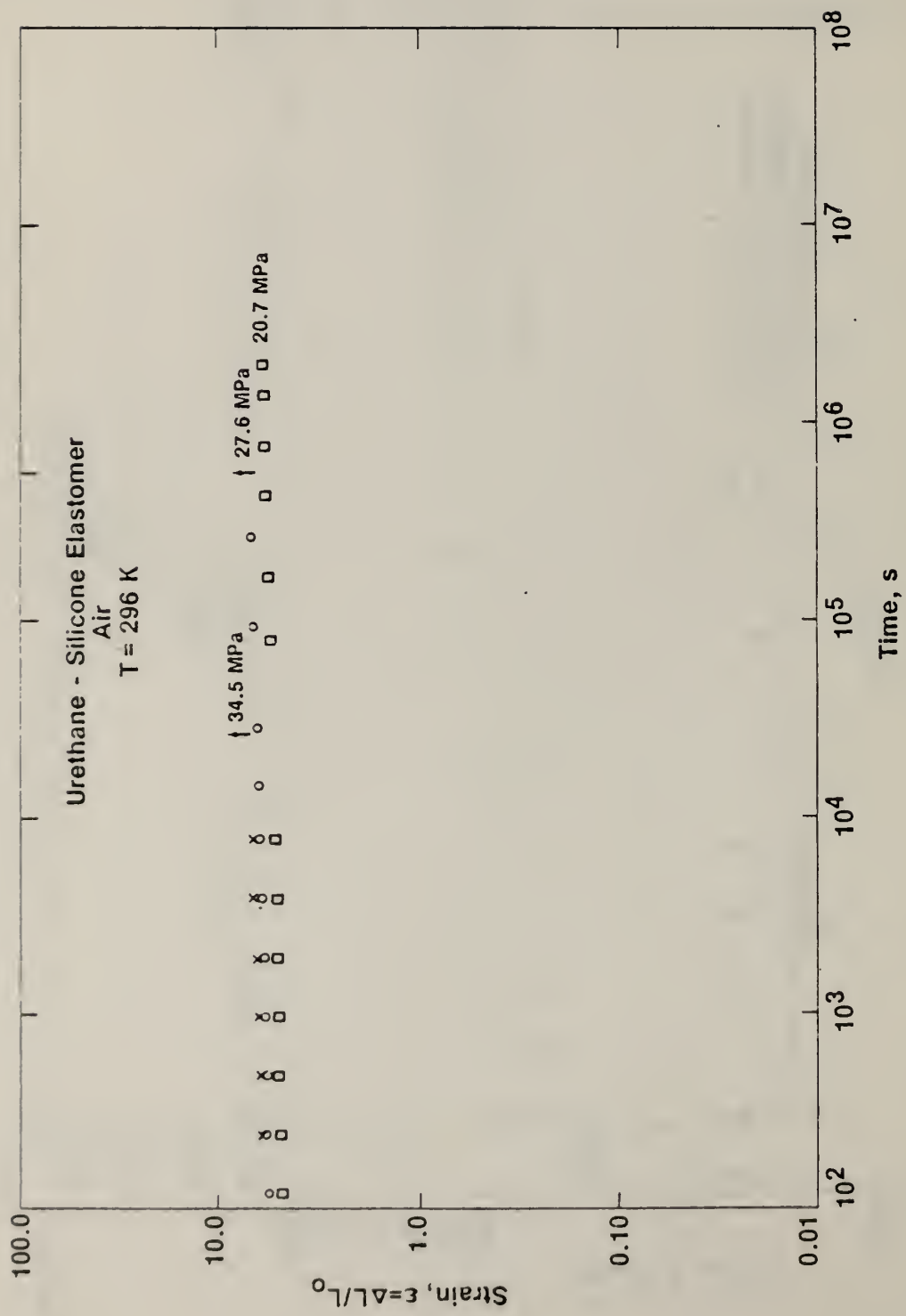
Figure 21. Uniaxial Creep of Urethane-Silicone Copolymer. In Air at 23°C.
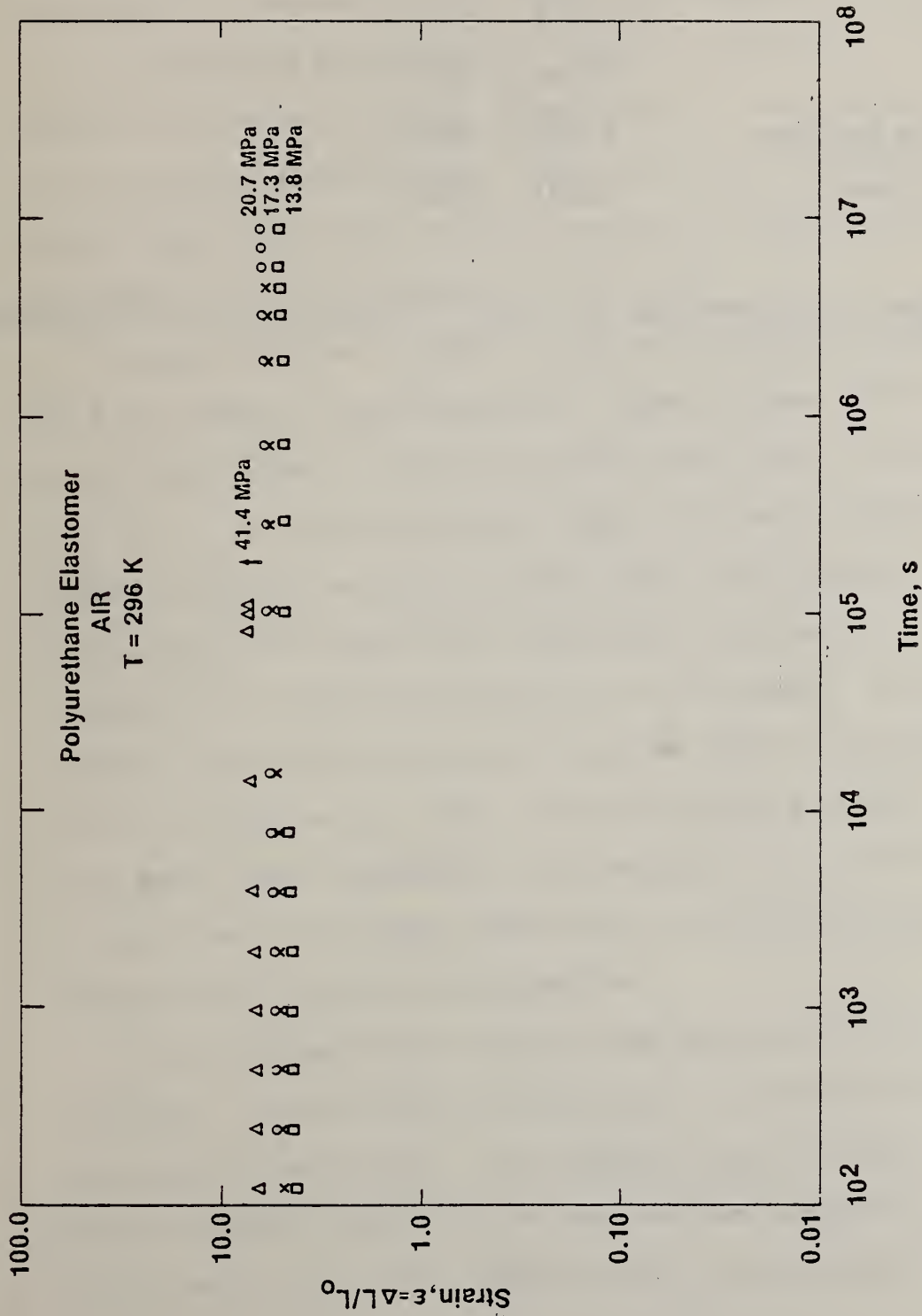
Figure 22. Uniaxial Creep of the Segmented Polyurethane Elastomer. In Air at 23°C.

TABLE 6

CREEP EXPONENT, n, FOR ELASTOMERS IN UNIAXIAL CREEP

ELASTOMER	n*
NBS Butyl	$0.0339 \pm .0055$
Polyolefin	$0.0399 \pm .0055$
Urethane-Silicone Copolymer	$0.0208 \pm .0058$
Polyurethane Elastomer	$0.0177 \pm .0025$

*From least squares fit of form $\ln \varepsilon = A + n \ln t$. Average value for all measurements

membrane (grips) the state of deformation is one of pure shear. Analysis of the inflated membrane is complicated by the fact that the stress at the pole of the membrane is dependent not only on the pressure and deformation (as measured by the stretch, λ) at the pole, but also on the radius of curvature of the inflated "bubble". The radius of curvature depends on the material modulus values as well as the internal pressure and varies with time during the test. Thus, for a simplified data presentation, we have chosen to use the internal pressure, p, divided by the membrane thickness, h, as our "engineering stress", p/h.

Our work, to date, has been limited to the polyolefin rubber and the NBS Butyl rubber at room temperature. Figure 23 shows typical behavior for the butyl rubber. Unlike the uniaxial data, which is nearly straight on a log ε - log t plot, the butyl rubber data shows a curvature upwards towards the end of the plot in biaxial creep. Also, there is considerably more scatter in the data than in the uniaxial case due to the imprecision of measurement of the strain at the pole of the sample. In spite of the curvature, we decided to fit a least squares line of the form $\ln\varepsilon = A + n\ln t$ as we did for the uniaxial data. Since the curves are nearly parallel and the exponent n was independent of the magnitude of p/h, we averaged the data and found that n is 0.0908 $\pm$ .0160 which is considerably greater than the value obtained in uniaxial creep testing.

Figure 24 shows typical biaxial creep behavior for the polyolefin elastomer. In this instance, the data plot in relatively straight lines, but are not parallel. This indicates that the creep rate is dependent on p/h. Figure 25 shows how the creep exponent, n, varies with the magnitude of p/h. Although there is considerable variability

41
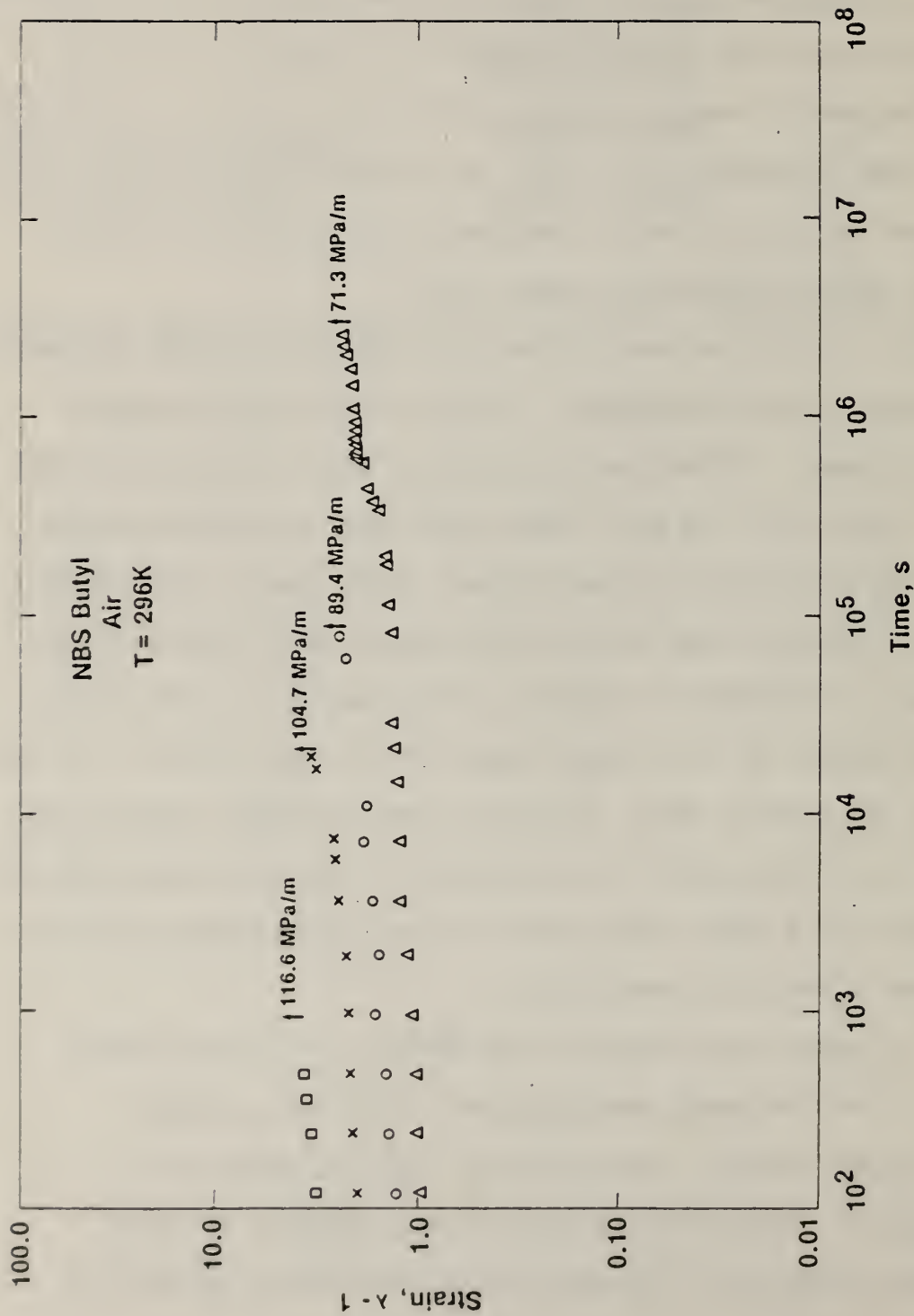
Figure 23. Equi-biaxial Creep of NBS Butyl Rubber. In Air at 23°C.

42
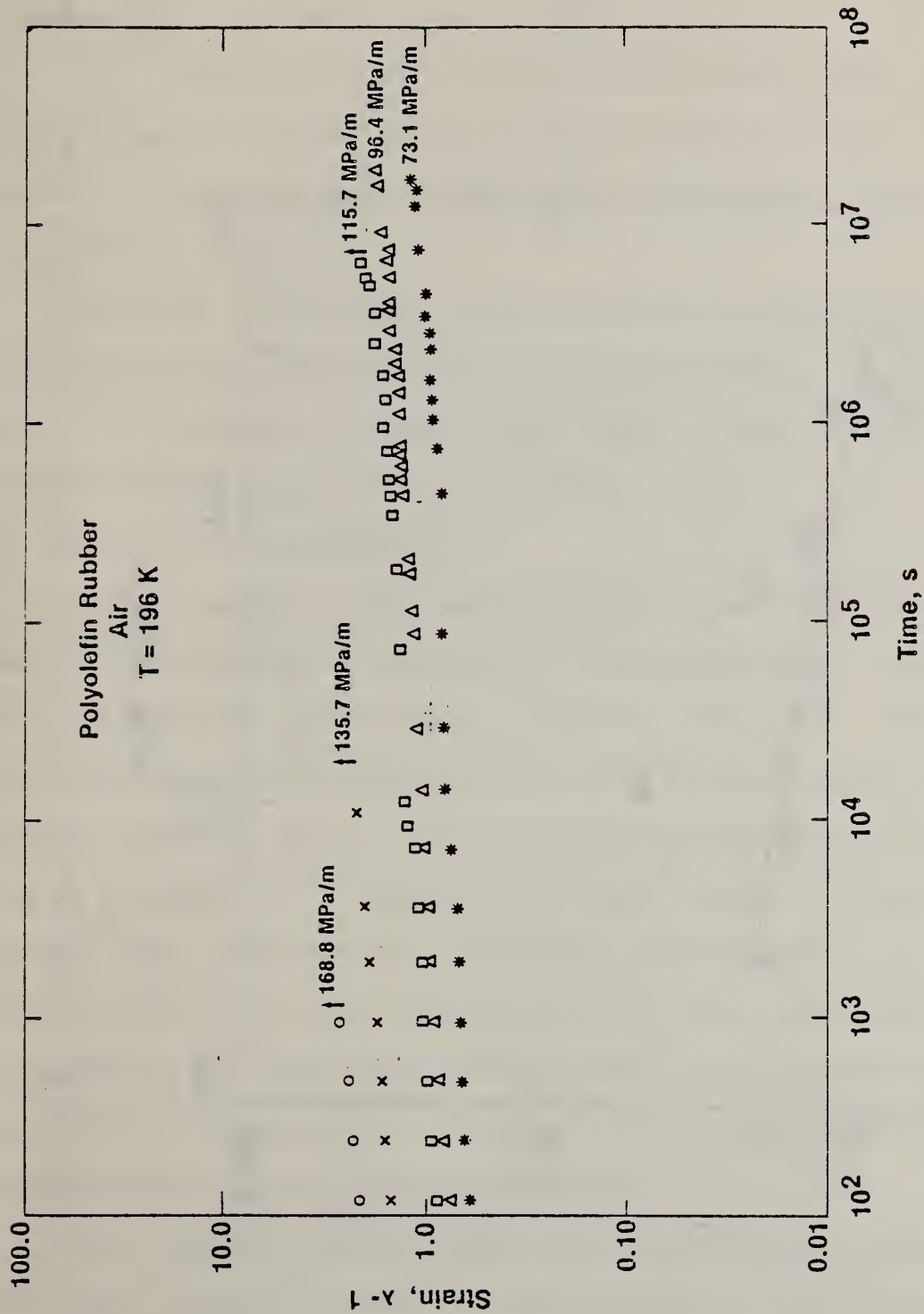
Figure 24. Equi-biaxial Creep of Polyolefin Rubber in Air at 23°C.
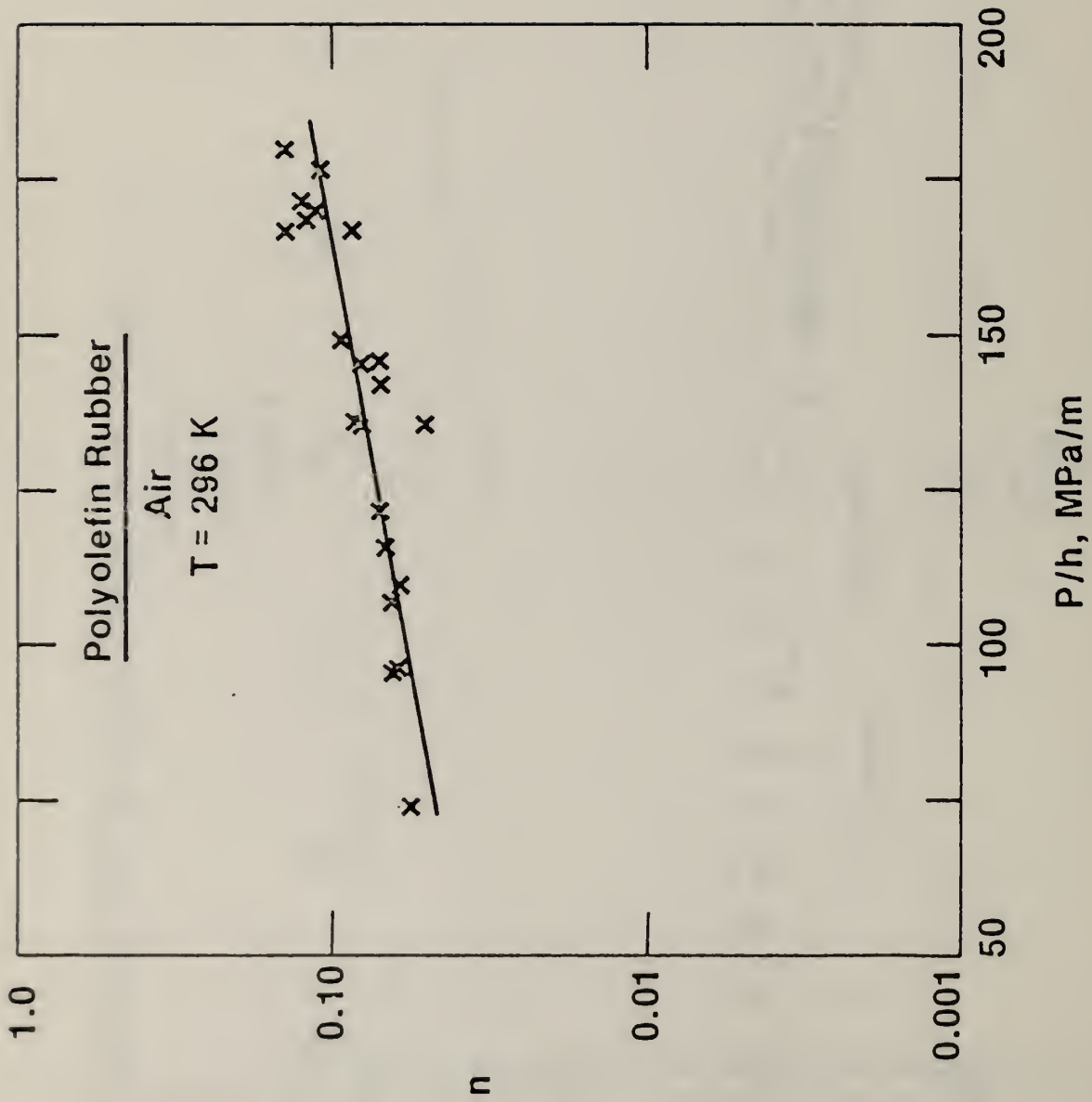
Figure 25. Creep Exponent vs. Reduced Pressure for Polyolefin Rubber in Equi-biaxial Stress. In Air at 23°C.

44

in the data, a line of the form $\ln(n) = 0.0262 + .00819 \, (p/h)$ fits the data quite well. Note that at the lowest values of p/h, the n is approximately 0.05 while at the higher p/h values n is approximately 0.14. This compares with the uniaxial value of 0.0399.

It is interesting to note that both the polyolefin rubber and the butyl rubber creep faster under equi-biaxial stress than under uniaxial stress, and points up that, in pump design, such phenomena should be taken into consideration.

During the upcoming year, this work will be extended to cover the urethane-silicone copolymer and polyurethane elastomers. In addition, work will be performed to study creep of the blood pump elastomers at higher temperatures and in saline solution.

D. Morphological Characterization

Evidence pointing to the manifestation of phase separation in the wall (200 μm thick) of an intra-aortic balloon made from a urethane-silicone copolymer was discussed in an earlier report (2). This earlier work suggested that phase separation on a scale coarse enough to be readily detectable under a light microscope at relatively low magnifications may be a characteristic feature of the type of urethane-silicone copolymer used in heart assist devices. Accordingly, the urethane-silicone copolymer sheets (625 μm thick) used in the mechanical testing program described elsewhere in this report were examined under an optical microscope. The observations described below illustrate the heterogeneous nature of the internal structure of these copolymer sheets.

Both transverse cross-sections, cut at right angles to the plane of the sheets, as well as thin slices cut parallel (or closely parallel) to the plane of the sheets were examined under a light microscope using

45

conventional transmission optics. The transverse cross-sections and the aforementioned slices were approximately ∿100 μm thick.

The photomicrograph (magn. x100) in Fig. 26 illustrates a transverse cross-section of a sheet. The letters A and B in that figure identify respectively reference points situated at, or very near to, the upper and lower surfaces of the sheet. The corresponding points are identified in Figs. 27,28 which show portions of Fig. 26 as they appear at a higher magnification (magn. x250). The regions depicted in Figs. 27,28 respectively were photographed in each case at two different levels of focus. The photomicrograph in Fig. 29 illustrates a portion of a slice which was cut essentially <u>parallel</u> to the plane of the copolymer sheet; the arrows in this figure delineate the edges of the slice which was somewhat thinner in the lower right hand region than elsewhere.

Heterogeneities of varying sizes may be seen dispersed throughout all the sample regions shown in Figs. 26-29 in which, due to the thickness of the samples, all the heterogeneities are not in focus. It is evident from these micrographs that phase separation occurs on a gross scale during the preparation and (manufacture) of the copolymer sheets and that the sheets consist of a matrix throughout which regions of another phase are dispersed. The chemical composition of the matrix and dispersed phases in these sheets is not known. Although the regions of the dispersed phase vary in size, Figs. 26-29 clearly reveal that all regions of this phase exhibit a similarity in shape, namely their appearance corresponds roughly to that of squashed spheres which are oriented with their largest dimension (corresponding to the diameter of the circular profile of the squashed spheres) parallel to the plane of the sheet. Deduction of the shape of the regions of the dispersed phase and the orientation of these regions relative to the plane of the sheet is based on (a) the characteristically

46
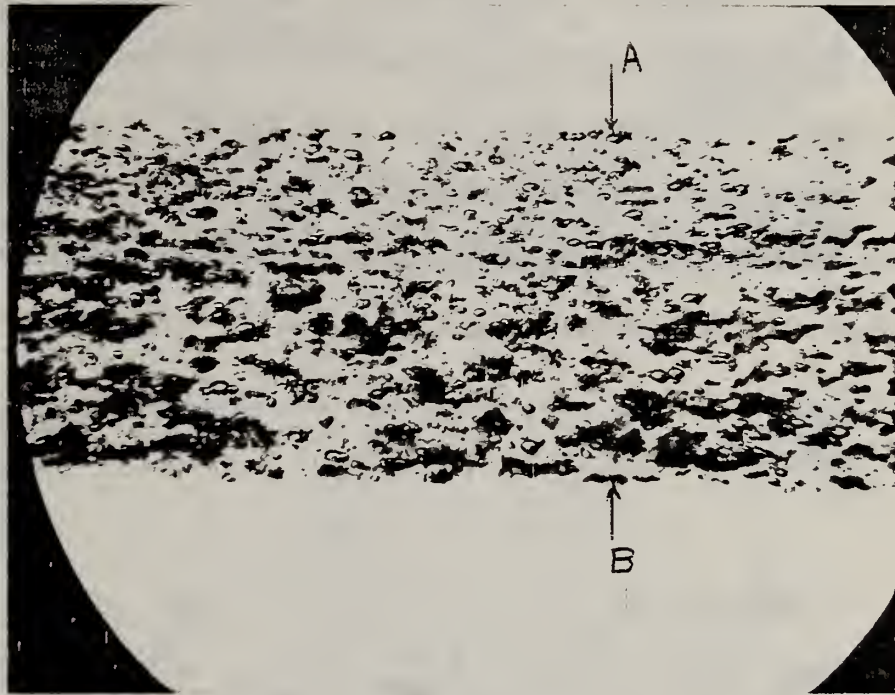
Figure 26: Transverse cross-section of a urethane-silicone copolymer sheet as seen under a light microscope using conventional transmission optics. Letters A and B identify points situated near opposite surfaces of the sheet. These points correspond to the similarly denoted ones in Figs. 27, 28. Even at this low magnification, elliptically shaped heterogeneities of varying sizes can be discerned over the whole cross-section. These heterogeneities are all oriented with their long axis parallel to the plane of the sheet (horizontal in the field of view). Magn. x100.

elliptical profile exhibited by the heterogeneities seen in transverse cross-sections in which these heterogeneities are characteristically oriented with their long axes parallel to the plane of the sheet (see <h> in Figs. 27,28), and on (b) the circular or essentially circular profiles exhibited by the heterogeneities when they are examined along an axis perpendicular to the plane of the sheet (Fig. 29).

The diameters of the squashed-sphere-like shaped regions of the dispersed phase, i.e. their sizes parallel to the plane of the sheets vary widely from a few micrometers up to ∿ 30μm. The average elliptical aspect ratio [long axis (i.e. diameter)/short axis] exhibited by the regions of the dispersed phase specifically identified (<h>) in Fig. 27 is ∿ 2.1.
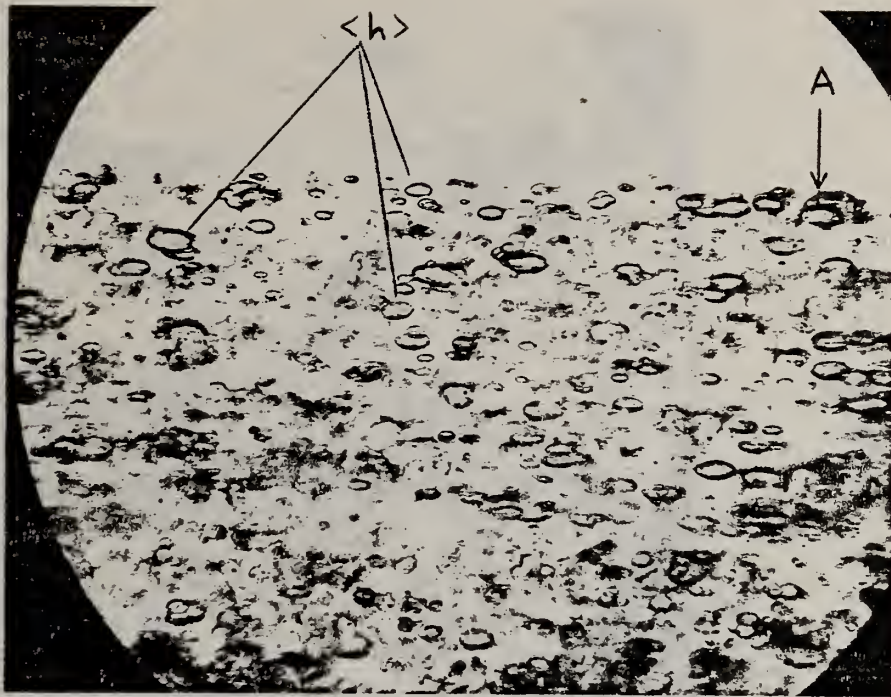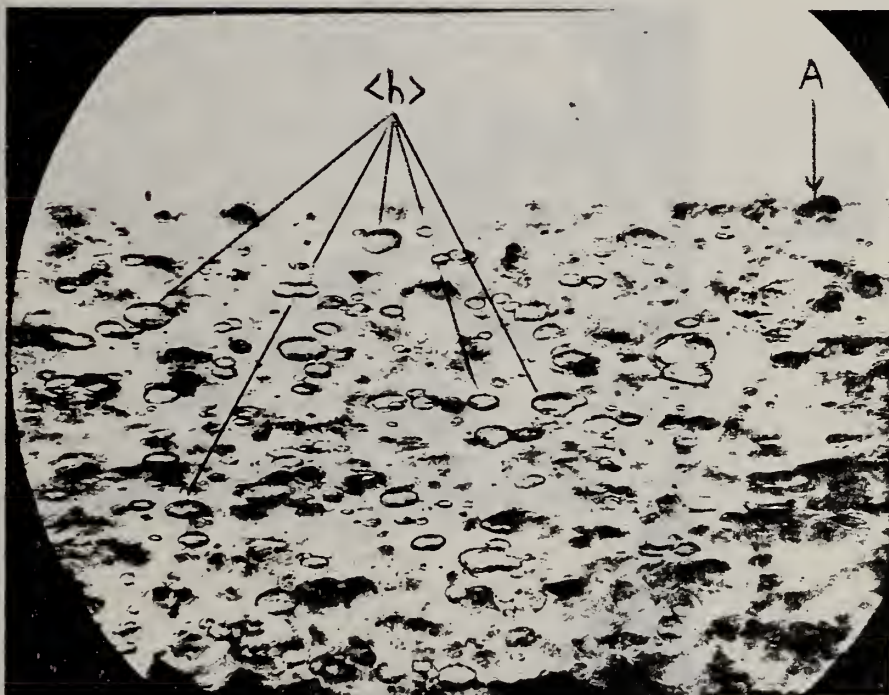
Figure 27: Portion of the transverse cross-section of the urethane-silicone copolymer sheet shown in Fig. 26 as seen at a higher magnification. The arrow A in each of the above figures serves to identify the area shown in relation to the corresponding area in Fig. 26. (a) and (b) were recorded at different levels of focus. Note the essentially elliptical shapes exhibited by the heterogeneities <h> which vary in size and which are oriented with their long axis parallel to the plane of the copolymer sheet. Magn. x250.
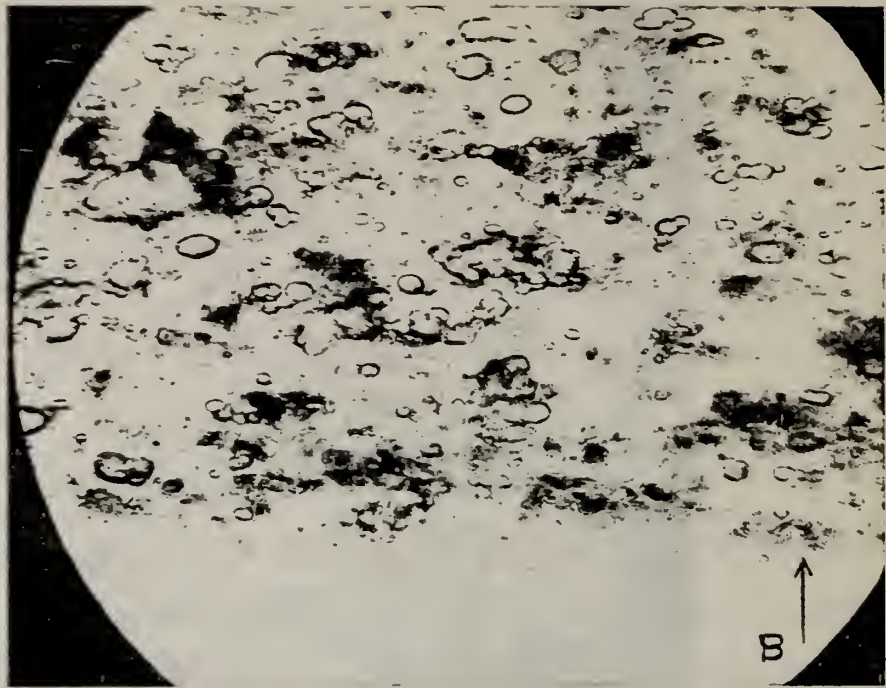
(a)
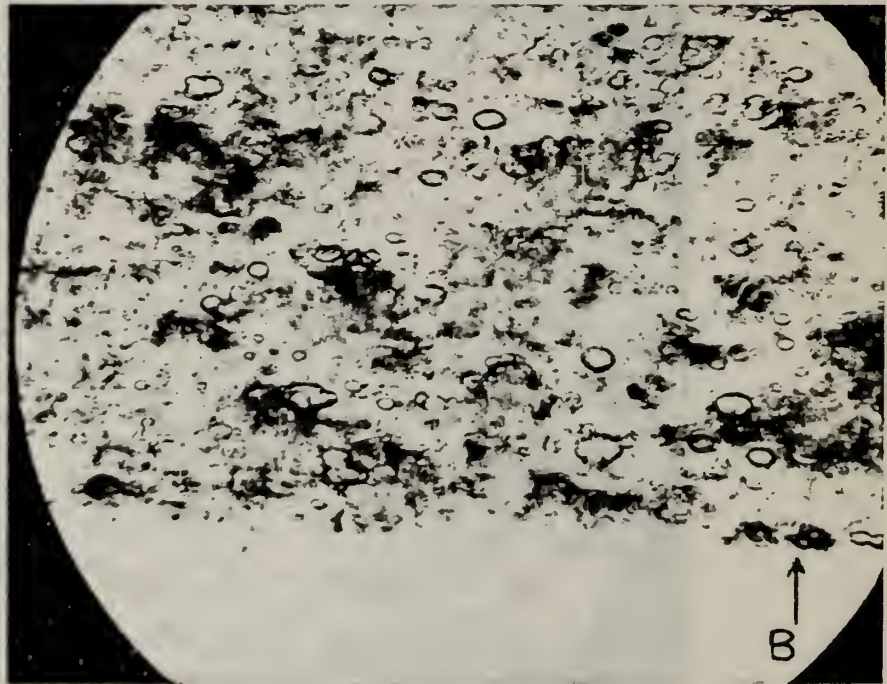
(b)

Figure 28: Portion of the transverse cross-section of the urethane-silicone
copolymer sheet shown in Fig. 26 as seen at a higher magnification.
The arrow B in each of the above figures serves to identify the
area shown in relation to the corresponding area in Fig. 26. (a)
and (b) were recorded at different levels of focus. Note the
essentially elliptical shapes exhibited by the heterogeneities
which vary in size and which are oriented with their long axis
parallel to the plane of the copolymer sheet. Magn. x250.
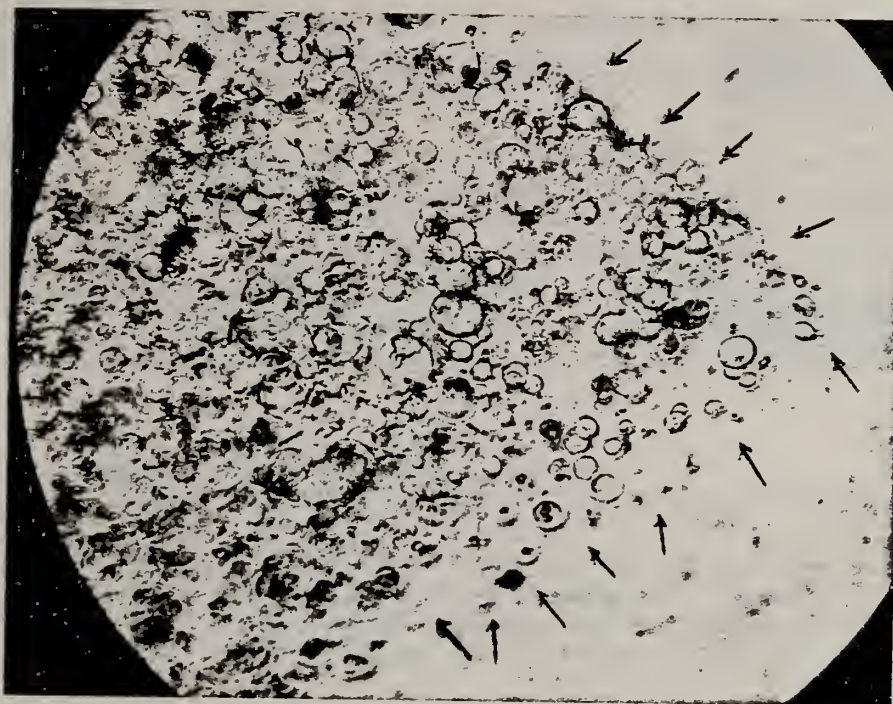
Figure 29: Portion of a slice cut <u>parallel</u> to the plane of the same urethane-silicone copolymer sheet from which the transverse cross-section shown in Figs. 26 to 28 was obtained. The arrows delineate the edges of the slice. Note the circular or essentially circular profile of the heterogeneities.

References

(1) McKenna, G. B. and Penn, R. W., "Time Dependent Failure Behavior of Poly(methyl methacrylate) and Polyethylene", Polymer (in press).

(2) Penn, R. W. and McKenna, G. B., "Physical Testing of Polymers for Use in Circulatory Assist Devices", First Annual Report, July, 1978, NBSIR #79-1741.

(3) Penn, R. W. and McKenna, G. B., "Fatigue Effects in Poly(methyl methacrylate) in Durability of Macromolecular Materials, ed. by R. K. Eby, ACS Symposium Series, 95, ACS, Washington, D. C., 1979.

(4) Bailey, J., "An Attempt to Correlate Some Tensile Strength Measurements on Glass: III", Glass Industry, 20, 94 (1939).

(5) Wood, L. A., Bullman, G. W. and Roth, F. L., "Long-Time Creep in a Pure-Gum Rubber Vulcanizate: Influence of Humidity and Atmospheric Oxygen", J. Res., NBS A, 78A, 5, Sept.-Oct., 1974, pp. 623-629.

NBS-114A (REV. 9-78)

U.S. DEPT. OF COMM. BIBLIOGRAPHIC DATA SHEET	1. PUBLICATION OR REPORT NO. NBSIR 80-2008	2. Gov't Accession No.	3. Recipient's Accession No.

4. TITLE AND SUBTITLE	5. Publication Date
PHYSICAL TESTING OF POLYMERS FOR USE IN CIRCULATORY ASSIST DEVICES	March 1980
	6. Performing Organization Code

7. AUTHOR(S) Penn, R. W., McKenna, G. B., Khoury, F. A.	8. Performing Organ. Report No.

9. PERFORMING ORGANIZATION NAME AND ADDRESS	10. Project/Task/Work Unit No.
NATIONAL BUREAU OF STANDARDS DEPARTMENT OF COMMERCE WASHINGTON, DC 20234	11. Contract/Grant No.

12. SPONSORING ORGANIZATION NAME AND COMPLETE ADDRESS (Street, City, State, ZIP)	13. Type of Report & Period Covered
Devices and Technology Branch Division of Heart and Vascular Diseases National Heart, Lung and Blood Institute National Institutes of Health/Bethesda, MD 20014	14. Sponsoring Agency Code

15. SUPPLEMENTARY NOTES

☐ Document describes a computer program; SF-185, FIPS Software Summary, is attached.

16. ABSTRACT (A 200-word or less factual summary of most significant information. If document includes a significant bibliography or literature survey, mention it here.)

The mechanical durability of an elastomer is a critical factor in its suitability for blood pump applications. In such applications, an elastomeric bladder is expected to undergo cyclic stress or strain histories at a frequency of approximately 1 Hz for periods of several years. Test methodologies for characterizing the mechanical durability of such materials do not exist.

In this report, we describe a test methodology which we have developed for the characterization of the durability of elastomers which are candidate materials for blood pump applications. This framework is based upon a cumulative damage rule which we have used to describe the time dependent failure of glassy and semicrystalline polymers. Within this framework, we are in the process of studying the durability of a polyolefin rubber, a urethane-silicone copolymer elastomer and a segmented polyurethane elastomer which are candidate materials for blood pump applications. We have also prepared a standard butyl rubber to use for inter laboratory comparisons with other labs working on this contract.

The cumulative damage framework suggests that the testing protocol be designed to examine four aspects of material failure:(1)failure under static loads,(2)failure under dynamic loads,(3)frequency dependence of dynamic failure,(4)statistics of failure. We report on our results to date on the uniaxial and equibiaxial failure of the blood pump elastomers using a testing protocol which includes the above four points.

17. KEY WORDS (six to twelve entries; alphabetical order; capitalize only the first letter of the first key word unless a proper name; separated by semicolons)

Elastomers; blood pump materials, biomaterials, urethane-silicone copolymer; Butyl Rubber; segmented polyurethane; time dependent failure; polyolefin rubber.

18. AVAILABILITY ☒ Unlimited	19. SECURITY CLASS (THIS REPORT)	21. NO. OF PRINTED PAGES
☐ For Official Distribution. Do Not Release to NTIS	UNCLASSIFIED	61
☐ Order From Sup. of Doc., U.S. Government Printing Office, Washington, DC 20402, SD Stock No. SN003-003-	20. SECURITY CLASS (THIS PAGE)	22. Price
☒ Order From National Technical Information Service (NTIS), Springfield, VA. 22161	UNCLASSIFIED	$7.00

USCOMM-DC